ABSTRACT

This study investigates the use of RAPRENOx, a non-catalytic selective reduction technology, to reduce nitrogen oxides in exhaust from a simulated gas turbine exhaust. The simulated gas turbine reactor was constructed to simulate gas turbine exhaust in order to test the effects of temperature, exhaust composition, and means of injection on the process. In addition, a new technology for the reduction of nitrous oxide in exhaust streams was demonstrated and the modeling of the technology was completed using a rigorous kinetic model. Incorporating an existing model for HNCO chemistry to test the ability to reduce nitrous oxide emissions resulting from the use of cyanuric acid in gas turbine exhaust further extended this model. The major accomplishments of this project include testing cyanuric acid injection in a simulated gas turbine exhaust where 80 % reduction was achieved, development of a N_2O reduction technology, and testing the effects of reactor design on results.

TABLE OF CONTENTS

LIST OF TABLES

LIST OF FIGURES

1.O BACKGROUND

With the major emphasis on meeting the goal of the 1990 Federal Clean Air Act, strict restrictions on new sources of nitrogen oxide emissions will be enforced in those areas that presently do not meet federal standards for air quality. These restrictions may impact on our nation's ability to drill for oil on offshore oil platforms where environmental concerns have already made oil exploration more difficult. The use of gas turbines on off-shore oil platforms accounts for approximately 65% of the NO_x emitted during oil exploration. Thus, a safe, cost-effective, reliable NO_x control technology for gas turbines is needed to aid in minimizing the impact of pollution control on our ability to drill for oil.

RAPRENOx, a patented process currently being commercialized in Diesel engines, promises to be suitable for this type of application. The process uses isocyanic acid, formed by the thermal decomposition of cyanuric acid, a non-toxic, nonflammable, commercially available solid material. The gaseous isocyanic acid, derived from cyanuric acid added to the exhaust stream reduces the NO to N_2, N_2O, H_2O and CO_2. In tests using three different Diesel engines, RAPRENOx has demonstrated 95% NO_x reduction.(1) Thus, this technology appears well suited for Diesel engine applications found on off-shore oil platforms.

This development program demonstrated that it is possible to reduce nitric oxide in a gas turbine while also reducing the nitrous oxide formed from the use of isocyanic acid. We investigated the effects H_2O, the use of natural gas, exhaust temperatures and reactor design (mixing) and we developed a comprehensive model to predict the use of a combined technology (HNCO/NaOH) to reduce both NO and N_2O in exhaust.

2.0 TECHNICAL APPROACH:

A research program, consisting of a combination of experimental and modeling efforts, was conducted to further characterize, develop, and assess the RAPRENOx process for NO_x control in gas turbines. The major goal of this research was to develop the necessary understanding of the chemistry to evaluate and implement the process. As part of this research effort a number of tasks were undertaken to reach the objective of our first demonstration in a gas turbine.

The first task was the construction of a model gas turbine test stand which enabled us to simulate combustion phenomenon in a laboratory environment. The model gas turbine reactor is discussed in section 3.3.

The second major task was to conduct experiments which tested ideas for reducing nitrous oxide (N_2O) using alkali metal additives. This work was completed using an existing multifuel-combustor operating on natural gas. The characteristics of this multifuel combustor is discussed in section 3.1 while the results of the testing are discussed in sec 5.1.

The third major task was to conduct laboratory-scale experiments using the model gas turbine test stand. The following parameters were tested:

1. Means of injection of cyanuric acid or isocyanuric acid
2. Oxygen sensitivity
3. Emissions from process
4. Reactor design

The experimental results are discussed in section 5.2.

The final task was to model both RAPRENOx and alkali metal nitrous oxide chemistry as a means to improve our basic understanding of both HNCO chemistry and alkali metal chemistry in combustion system. By comparing experimental results with the modeled projections we could gain insights to aid in engineering a practical system. We used computational facilities at Sandia National Laboratories for the calculations. This modeling effort provided the necessary theoretical framework to implement the chemistry and to test ideas with regard to nitrous oxide reduction resulting from the use of cyanuric acid. The model is discussed in section 6.0

3.0 TEST FACILITY:

The test facility at Technor is comprised of a multifuel-combustor-flow reactor and a model gas turbine test stand. The multifuel-combustor was used for the initial alkali metal/ N_2O experiments, and the model gas turbine test stand was used for testing of cyanuric acid.

3.1 Multifuel Combustor (Nitrous Oxide Reduction Experiments):

A summary of the operating parameters of the multifuel combustor is listed in Table I. The down fired combustor as composed of three primary regions, a combustion zone, a venturi zone and a reaction zone. The multifuel combustor was used to test ideas for reducing nitrous oxide. Nitrous oxide was added to the exhaust from the combustion zone in order to raise the initial concentration of nitrous oxide in the exhaust. In addition, alkali metal/water/air or water/air mixtures were injected into the exhaust using a simple air brush, modified to mount on an existing flange. Propane was added to the venturi region. This exhaust mixture was sampled at the bottom of the reaction chamber. The concentration of the nitrous oxide was determined from prior calibrations using the FTIR and was compared to calculated nitrous oxide concentrations based upon known gas flows. The results of these experiments are discussed in section 5.1.

Table I. Combustor Operating Parameters

Operating Parameters	Range	Baseline
Firing Rates:	70-350 kbtu/hr	150 kbtu/hr
Combustor Flow Rates:	15-70scfm	22 scfm
Test Section Velocity:	5-33 ft/sec	8 ft/sec
Test Section Temps:	400-1400 °C	600 °C
Residence Times:	0.5-1.0sec	1.0 sec
Test Sec. Reynolds No.:	1,000-10,000	2,200

3.2 Gas Analysis System:

Figure 1 shows the gas analysis systems schematic used for both the alkali metal/ N_2O experiments and the RAPRENOx experiments. Gaseous and solid samples are obtained from the combustor using a water cooled gas quench probe. A thimble separates the solids while the gas sample is transported to the gas analyzers through a heated Teflon sample line. The sample is analyzed for O_2, CO_2, CO, and NO_x using the equipment listed in Table II.

Besides the instrumentation listed in Table II, a Mattson Polaris FTIR with a 6 meter multipass gas cell was used to characterize the exhaust. This instrument has a high sensitivity for such gas species as HNCO, N_2O, NH_3, HCN, CO, and CO_2. This system allows for the simultaneous detection of a wide variety of infrared active species with a sensitivity better than 1 ppm in ideal conditions and practical sensitivities of 5-10 ppm in combustion environments.

Table II. Gas Analysis Instrumentation

Species	Analyzer	Range*
O_2	Teledyne Model 326RA	0 - 5%
		0 - 10%
		0 - 25%
CO	Horiba Model PIR 2000	0 - 500 ppm
		0 - 1500 ppm
		0 - 2500 ppm
CO_2	Horiba Model PIR 2000	0 - 5%
		0 - 15%
		0 - 25%
NO/NO_x	TECO Model 14BE	0 - 50 ppb
		0 - 100 ppb
		0 - 200 ppb
		0 - 500 ppb
		0 - 1 ppm
		0 - 2 ppm
		0 - 5 ppm
		0 - 10 ppm**

* Selected concentration range. Sensitivity resolution better than 2% full scale.
** Extended to higher ranges using diluted flows with mass flow meters.

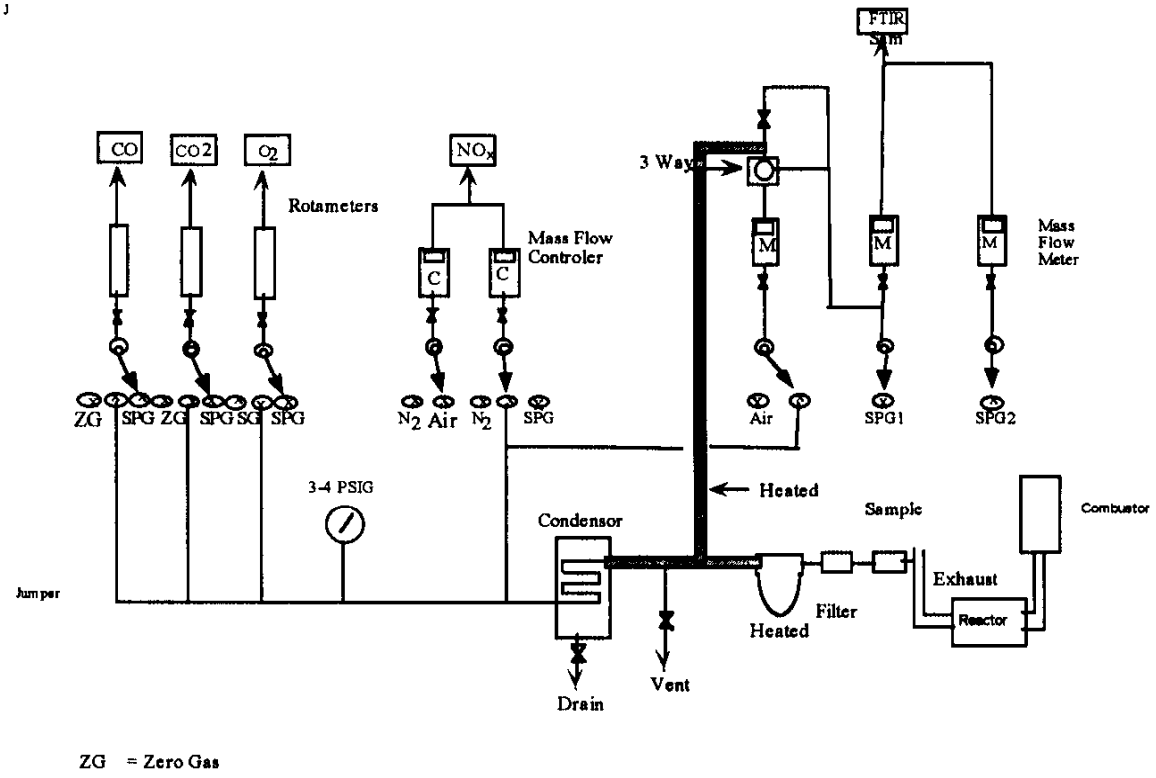

ZG = Zero Gas

Figure 1: Gas analysis system schematic.

3.3 Model Gas Turbine Test Stand:

The model gas turbine test stand is comprised of three regions, 1) the model gas turbine, 2) the injection region just beyond the gas turbine and 3) the reactor zone. During the course of the study changes were made to the injection region and reactor zone to improve and test different configurations.

Atmospheric Model Gas Turbine:

The atmospheric model combustor was designed to retain the important features found in conventional gas turbine combustors while permitting flexible operating conditions. Essentially, fuel is centrally injected into a tube (combustor liner). Surrounding the fuel injector is an aerodynamic swirler which provides a recirculation zone to stabilize the reaction. A step or angled expansion provides the transition from the outside diameter of the swirler to the combustor liner wall. Air passes through the liner in discrete jets which serves to enhance mixing, tailor recirculation zone size and provide cooling of the exhaust prior to entrance into the turbine. Based on input from engine designers, jet locations are selected at one and two combustor diameters downstream of the inlet. A row of jets is located one combustor diameter downstream of the inlet plane which mimics the primary jets in the actual combustor. These jets are designed to operate with an injection velocity of approximately 90 m/s. The role of these jets is to help provide closure to the recirculation zone which would otherwise extend beyond the end of the combustor. Another row of jets is located one combustor diameter downstream from the primary jets. These jets mimic the role of dilution jets in

the conventional combustor. These jets are used primarily to cool the exhaust products before they enter the turbine. A lower velocity (~ 60 m/s) with more flow is provided through these jets.

Based on design guidelines developed from input obtained by engine manufacturers, flow splits of 15% swirl, 37% primary jets, and 48% dilution jets are used. The combustor is designed to operate with an overall equivalence ratio of around 0.3. Based on assumptions about jet flow splits, this gives a recirculation zone equivalence ratio of about 0.7-1.0. Additionally, it is desired to maintain a reference velocity of at least 33 ft/s. The reference velocity is determined by the ratio of the total volumetric air flow to the cross sectional area of the combustor with the inlet temperature and pressures. In conventional combustors, the air flows through the swirler and liner are dictated by the pressure drop across the passages. This creates challenges for varying individual air streams. As a result, the present configuration provides individual metering of each air stream. This permits the effect of varying the flow splits to be evaluated in a straight forward fashion.

Technor's combustor has a 2.5" schedule 80 pipe which provides a reference velocity of about 33 ft/s with a conservative total air flow of about 60 SCFM. Using the flow splits and desired jet velocities, the jet diameters were established at 0.24 inches and 0.43 inches for the primary and dilution jets, respectively. The jets are configured to be interchangeable. As configured, natural gas is centrally injected through a cone annular nozzle with a 45-degree injection angle. Surrounding the nozzle is a 60 degree, 100% solidity swirler which creates a suitable recirculation zone. This design does allow for other nozzles or liquid fuel to be used with a substitution of the fuel tube.

A major effort was made to simulated a gas turbine exhaust. It was hoped that conditions could be established that represented a gas turbine exhaust with regards to temperature, O_2 concentration, H_2O, NO_x and flow conditions. The one major problem with this approach, not fully recognized until after much effort was expended, was the significant limitation of the low-pressure reactor. At low pressures complete combustion of the CO does not occur before quenching of the combustion with dilution air. While this is not a major problem when the low pressure combustor is used for studying mixing characteristics, it presents a major problem when trying to vary the fuel-air ratio because of the direct relationship between the combustion of CO, temperature, and fuel/air ratios. Practical problems with the operation of the model gas turbine, thus limited the dynamic range of operation of the combustor.

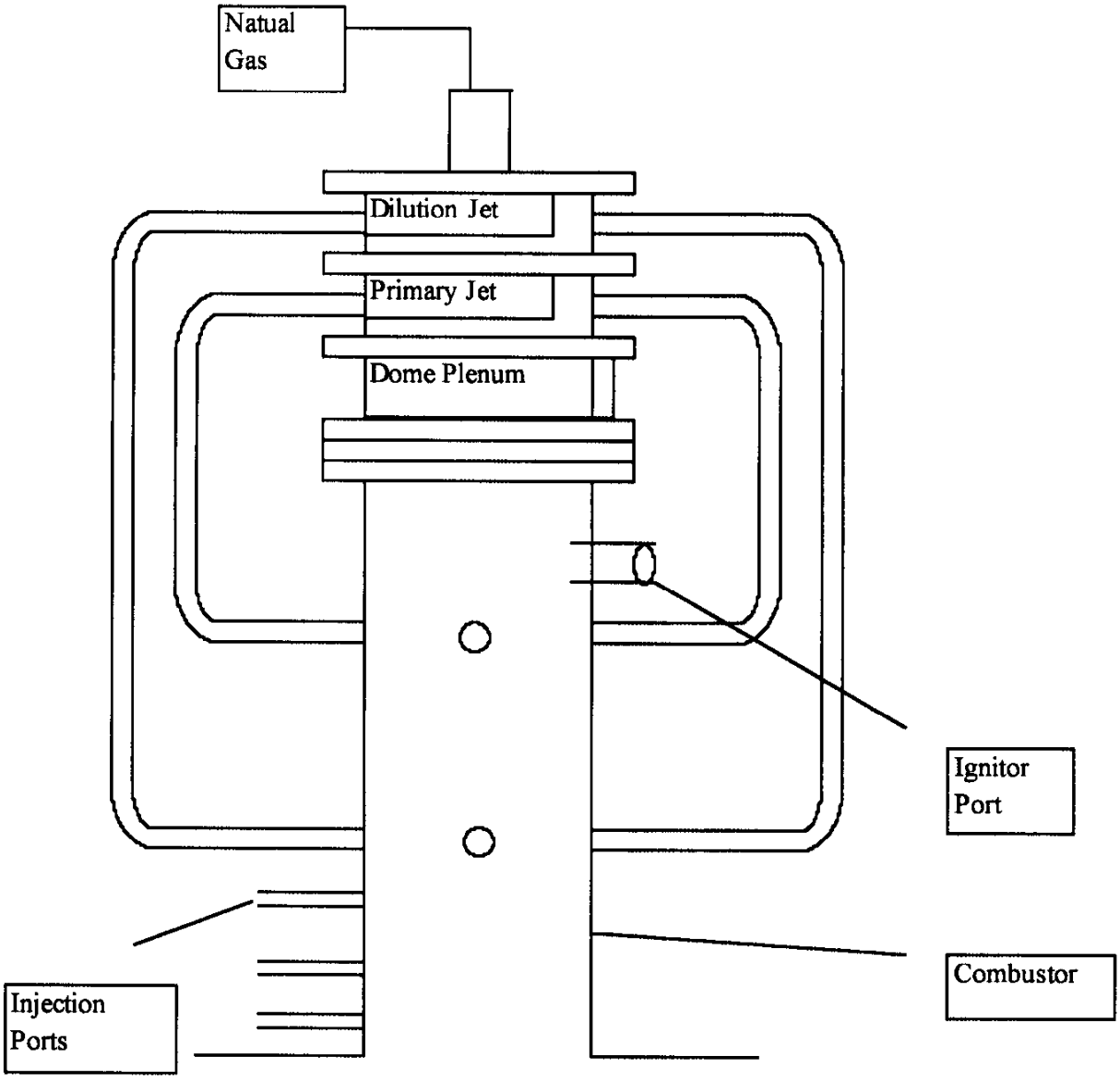

Figure 2. Schematic of Model Combustor

Reactor Zone:

We used our down-fired-multifuel combustor (the burner was replaced with the model gas turbine) in our initial experiments. Due to the difficulties in working with this configuration (14 feet up in the air) this system was redesigned and mounted on top of a table at room level. The new design was mounted vertically at table height while the reaction vessel (a 16" diameter by 30"

length) was mounted horizontally under the table. The reaction vessel provided a 0.6-1.0 second residence time and a recirculation zone to enhance the chemistry. In testing the reaction vessel a strong coupling of the operation of the model gas turbine and the restrictive design of the recirculation zone was noted. It was discovered that the restrictive diameters that gave "best " mixing conditions made the combustor unstable. The best solution to the unstable operation of the combustor was the final design where a variable plate was inserted one diameter downstream from the injection point. This system is seen in Figure 3. The results from this design are further discussed in section 5.2. Exhaust gas was sampled down stream from the reaction vessel prior to venting into existing ductwork.

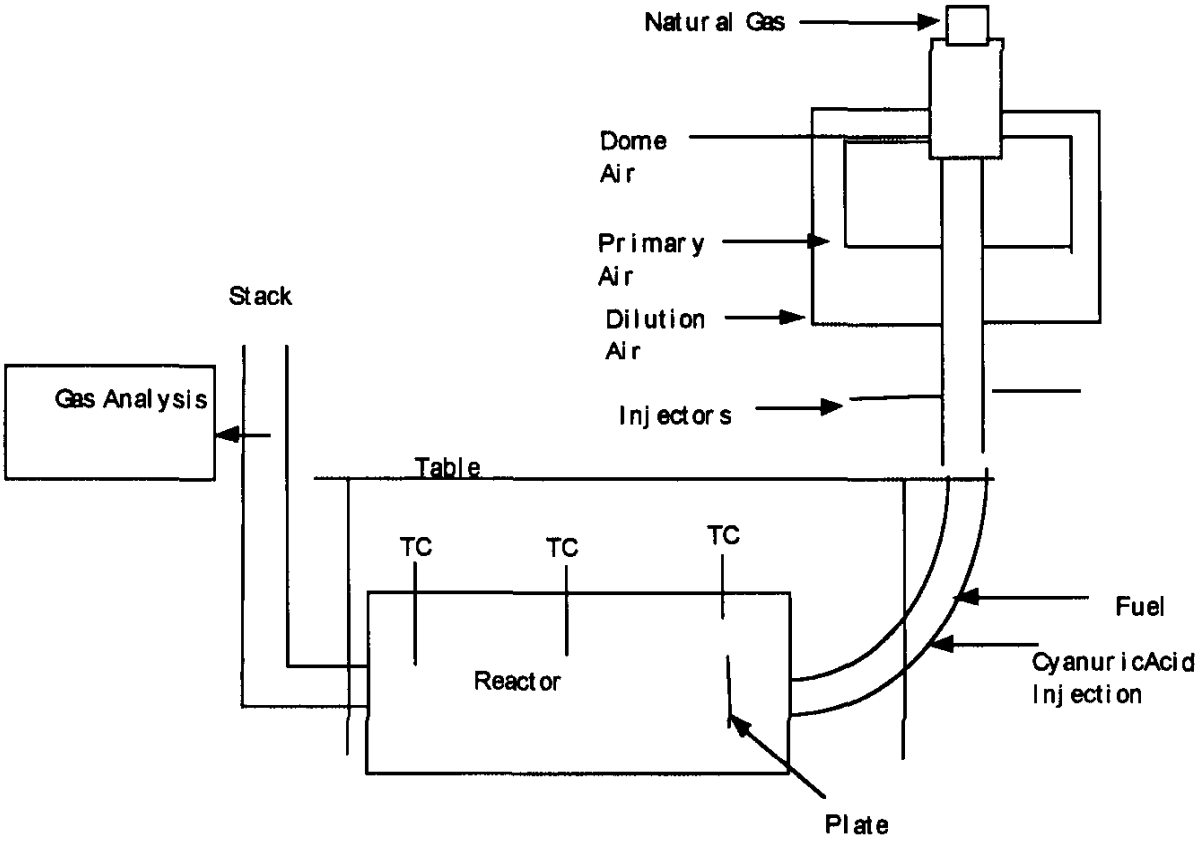

Figure 3. Flow diagram of model gas turbine test stand.

4.0 TECHNICAL APPROACH TO CYANURIC ACID EXPERIMENTS:

4.1 Cyanuric Acid/HNCO Acid Experiments:

Most of the experiments discussed utilized either a powder injection system incorporating a particle feeder with an eductor to inject solid cyanuric acid or a presublimed HNCO gaseous injection system similar to prior Diesel applications. In the gaseous injection system the particulate

cyanuric acid was fed through a duel synchronized valve arrangement into a temperature controlled heated chamber. Air flowing through the chamber carried the isocyanic acid into the exhaust derived from the model gas turbine. The HNCO injected was estimated based upon the calibrated cyanuric acid feed rates determine from the particle feeder.

4.2 Slurry Injection

Our work to design a slurry injection system to be used with Diesel injection was unsuccessful due to the small scale of the injection system. At the low flow rate required in our test system the injection nozzle proved to be too small to work reliably. Not only did we have problems with the slurry due to the plugging of the injectors but we also had problems with pyrolysis of the Diesel which caused plugging of the small orifice used for the Diesel injection. Out of this work an improved slurry injection system was devised for further study.

4.3 Fuels Tested

Tests were completed with various fuels used as a co-injection system to promote radical generation. While both Diesel and propane were interchangeable as a supplemental fuel the use of natural gas required higher initial temperatures for ignition or alternately the injection of Diesel of propane to enhance the initial ignition of the natural gas. (A natural gas duct burner design would eliminate this problem by increasing the initial temperature to correspond to the ignition temperature for natural gas.)

4.4 Steam Injection

Finally, test were run with water injection to raise the water concentration (to simulate steam injection). The water was injected using one of the dilution ports (see Figure 2) with the aide of an educator to enhance mixing of the water with the air. In this combustor the addition of water increased the CO concentration and made ignition of the supplemental fuel more difficult. If reactor temperature was raised prior to water injection it was possible to operate the system in a stable fashion.

5.0 EXPERIMENTAL RESULTS:

5.1 Nitrous Oxide Reduction Technology Experiments

One of the major achievements of this study was the demonstration of the effectiveness of NaOH as an additive for reducing N_2 O. Results show that it is possible to obtain very efficient reduction of N_2O in a lean exhaust at moderate temperatures. Besides NaOH, three other additives were tested and shown to be less effective. These additives are KOH, $Ca(OH)_2$ and Na_2O_2 . The experimental results for NaOH and KOH are listed in Table III and IV.

Table III N_2O reduction with NaOH added.

T(C)	N_2O (ppm)*	%** Reduction	NaOH*** (ppm)	O_2 %	CO (ppm)
750-780	165	.....	0	4.5	50
750-780	40	76	5.4	4.5	120
720-770	66	60	5.4	3.8	32
780-800	<5	100	5.4	3.0	32
722-753	536	.....	0	5.0	360
716-719	327	43	5	5	1200-2800
722	308	43	5	5	1100-1300
753-781	74	65	5	3.8	600
756-760	50	65	5	3.8	300
750	212	.....	0	3.8	40
780-803	60	72	5	3.8	<95

** N_2O concentration is measured using FTIR calibration data. Actual initial N_2O concentration is higher based upon flow rate measurements.*

*** Note the % reduction is based upon formula 1-(N_2O (final)/ N_2O(blank)) where N_2O blank is the measured* N_2O *concentration without NaOH added.*

**** The concentration of NaOH is calculated based upon flow rate and concentration data.*

The catalytic activity for the conditions studied was approximately 50-100/1. That is, one mole of Na effectively reduced 50 moles of N_2O. Under all conditions the best reduction of N_2O occurred concurrently with the most effective reduction of carbon monoxide.

Table IV N_2O reduction with KOH added.

T (C)	N2O*(ppm)	%** Reduction	KOH(ppm)** *	O2 (%)	CO (ppm)
740	145	-----	0	3	50
756-782	65	55	10	3	300
750-775	120	18	10	3	300
740	322	20	10	3	600-900
729-739	406	0	2	3	223

The ability of alkali metal additives to reduce N_2O was shown to be dependent upon the initial concentration of the alkali metal additive, upon the initial concentration of the N_2O, upon the temperature and upon the ability to sustain a combustion environment. In experiments where greater than 5 ppm of NaOH was added quenching of the CO combustion reduced the effectiveness of the additive for similar temperature and fuel addition. In experiments where the fuel was not injected no effect of addition of NaOH was observed. Also, at higher initial N_2O concentrations

additional metal additive was needed to obtain effective reduction. Based upon these experiments, LiOH would also be expected to be an effective additive and might be more effective than NaOH.

$Ca(OH)_2$ was not shown to be effective at the temperatures studied. Na_2O_2 was expected to be similar to NaOH, but due to the difficulty in feeding this material, and the fact that Na_2O_2 is a very strong oxidant, experiments were discontinued after only moderate success.

5.2 Injection of Cyanuric Acid/Isocyanuric Acid

Before the inclusion of a recirculating reactor experiments were completed to test the effect of injection of cyanuric acid to different areas of the gas turbine. When cyanuric acid was injected downstream from the MGT (model gas turbine) with additional fuel, quenching of the propane/air lean burn zone was observed.

Model Gas Turbine Injection

Cyanuric acid was injected into three locations of the MGT. Cyanuric Acid was injected into top of the MGT, bottom of the MGT and into the secondary air. Figure 4 and Table V shows the result of injecting cyanuric acid directly into the model gas turbine combustor.

Table V.

T (C)		CYA (g/min)	NOx (ppm)	CO (ppm)	O_2 (%)	% Reduction
832	*	0	210	22	12.5	--------
832	*	.54	190	47	12.5	10
832	*	1.0	160	52	12.5	24
832	**	0	225	29	12.7	--------
832	**	1.0	190	36	12.7	16
746	**	1.0	160	71	12	29
746	**	0	245	71	12	--------
746	**	1.0	205	53	13	16
784	***	0	210	28	13	--------
785	***	1.1	160	117	13	24
783	***	1.6	150	124	13	29
756	***	0	400	90	14.5	--------
756	***	.5	370	135	14.5	7.5
756	***	0	390	95	14.5	--------
756	***	5	310	350	14.5	22.5
757	***	2.5	340	350	14.5	15
716	***	0	540	80	13.5	--------
719	***	2.5	480	159	13.5	10.3

* Cyanuric acid particles injected at bottom of model combustor.
** Cyanuric acid particles injected at top of model combustor after secondary air.
*** Cyanuric acid particles injected with the secondary air.

With the addition of cyanuric acid directly into the model gas turbine combustor only a 25% reduction in NO_x was observed. This value contrasted with the very high efficiency (>90%) observed for Diesel applications and suggested the need to include a better reactor design for maximum efficiency. Figures 5 and 6 shows the effect of adding cyanuric acid directly to the secondary air. This was done in two ways. The first test were done with no fuel added downstream from the MGT. These tests produced increase CO with slight reduction in NO_x (Figure 6.) Following these test cyanuric acid was injection into the secondary air stream with the addition of 10% additional fuel (propane) added down stream from the MGT. While the region down stream from the MGT does not have a recirculation zone it was possible to observe secondary combustion of the propane with the CO_2 concentration rising by the corresponding amount representing the expected formation of CO_2 from the consumption of 10% propane (approximately 0.5%). While a slight improvement was observed with the addition propane it is apparent that the cyanuric acid is primary consumed in the high temperature region where the secondary air is introduced. Again a reaction region down stream from the turbine with a better defined recirculation zone is necessary based upon these results.

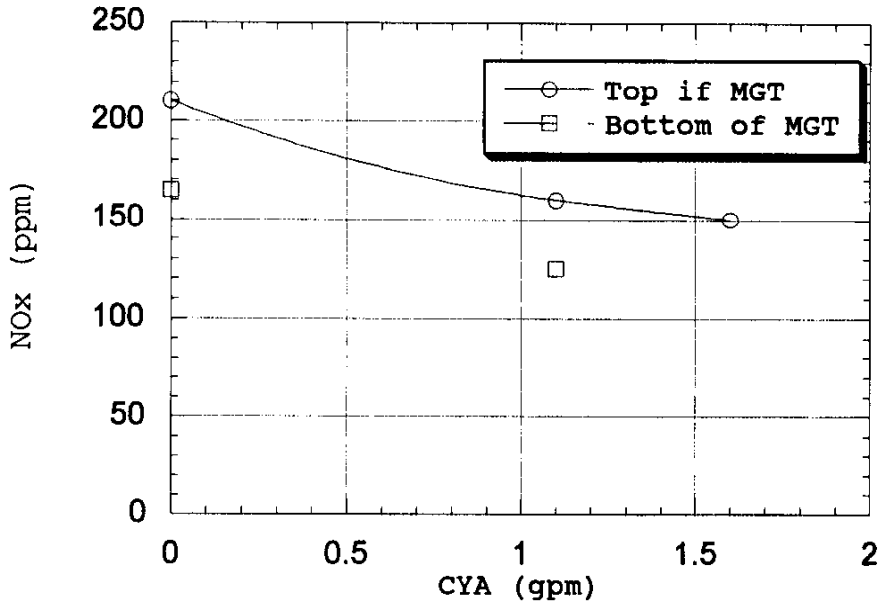

Figure 4. Cyanuric Acid injected into top and bottom of model gas turbine combustor.

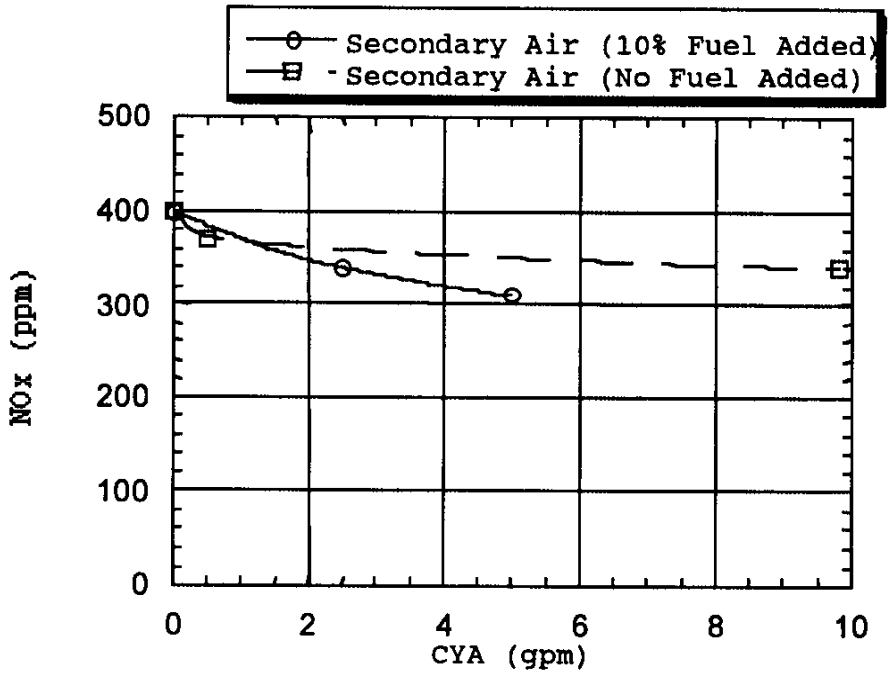

Figure 5. Cyanuric Acid Injected into secondary air of model gas turbine.

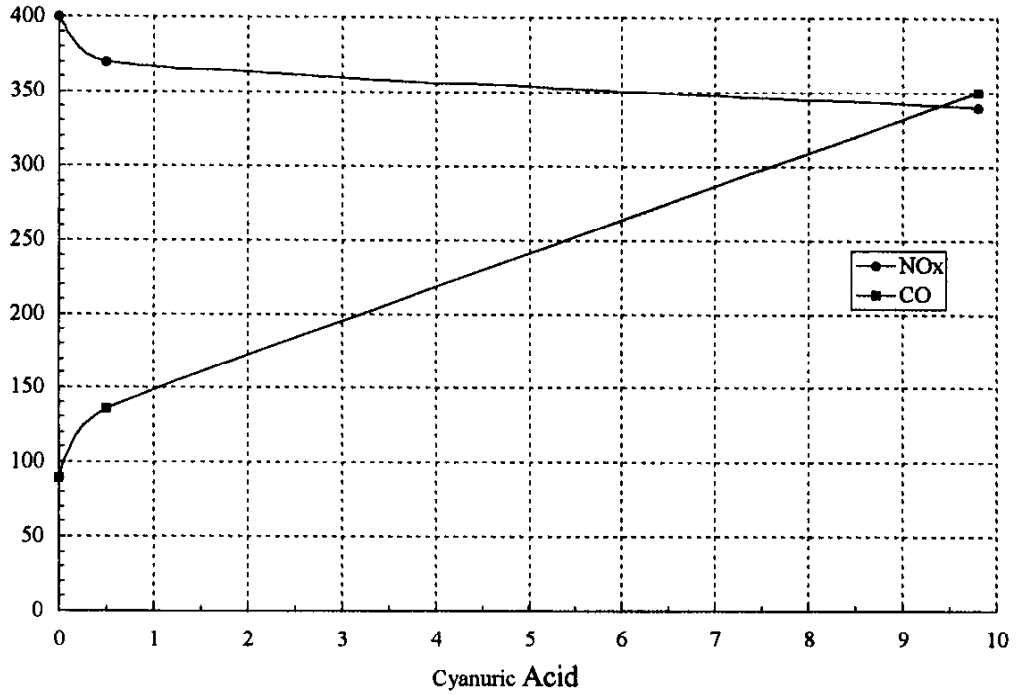

Figure 6. NO_x and CO concentration for addition of cyanuric acid to secondary air. No fuel added downstream.

As part of this program an effort was made to explore possible injection procedures for isocyanuric acid or cyanuric acid. Due to the importance of reacting HNCO with NO in the exhaust, efforts in the past had focused on conversion of cyanuric acid to HNCO prior to injection into the exhaust. As part of this program we have focused on developing an alternating injection scheme; one that injected cyanuric acid as a slurry or powder system while providing the reaction time needed for conversion of cyanuric acid in the exhaust. Our work to design a slurry injection system to be used with Diesel injection was unsuccessful due to the small scale of the injection system. At the low flow rate required in our test system the injection nozzle proved to be too small to work reliably. Not only did we have problems with the slurry due to the plugging of the injectors but we also had problems with pyrolysis of the Diesel which caused plugging of the small orifice used for the Diesel injection. Out of this work an improved slurry injection system was devised for further study.

Figure 7 shows results for injection of gaseous isocyanic acid into the final recirculating reactor. Very high reduction efficiency was obtained at 14.5% oxygen and 10% propane injection. Final temperature of the reactor is 720 C. While these results demonstrated the ability to obtain very good NO_x reduction using a recirculating reactor high levels of CO (300 ppm were observed at these temperatures. Efforts to lower both CO and NO_x simultaneously led us to conclude that a better design for the recirculating region was necessary.

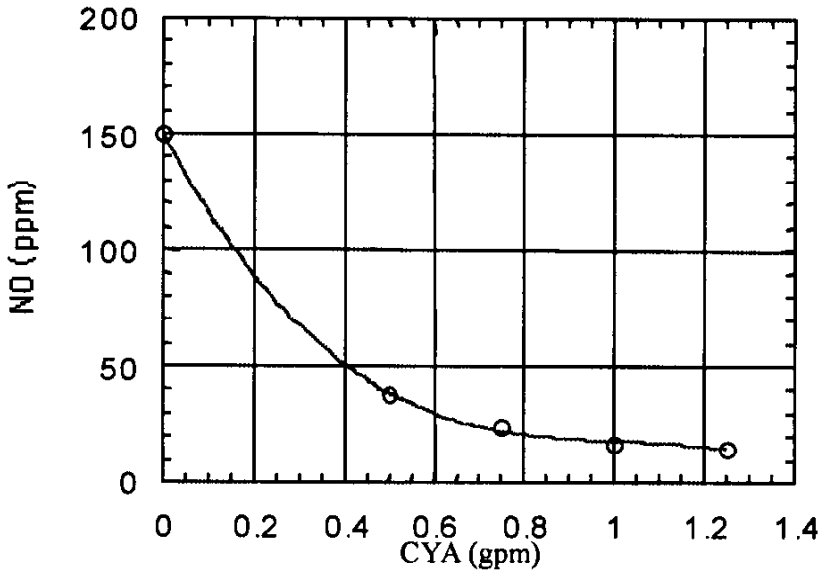

Figure 7: NO reduction with cyanuric acid as HNCO gas to recirculating reactor. 10% propane added as supplemental fuel. T=720 C.

Utilization of cyanuric acid to reduce NO_x in a gas turbine that already employs a steam injection system to lower the initial NO_x concentration led us to try using cyanuric acid at high (12%) water concentrations and lower oxygen concentrations. Results from these test are indicated in Figure 8. Note that the initial concentration of NO_x is limited to 70 ppm to represent the lower initial NO_x concentration found in a steam injected gas turbine. Under these conditions significant NO_x reduction was observed but the amount of cyanuric acid needed to reduce 41% of the NO_x corresponded to a CYA/NO_2 ratio of 4.

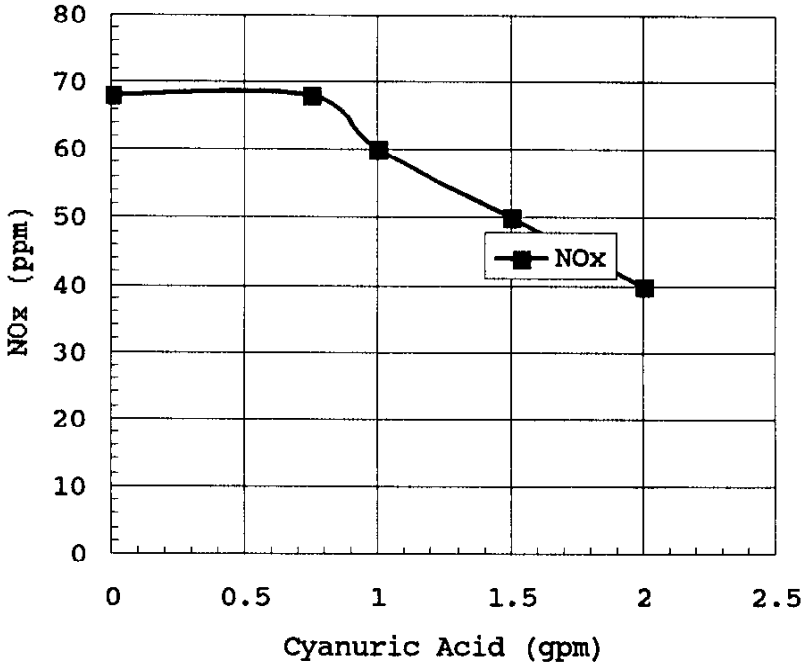

Figure 8. Cyanuric Acid Injected into exhaust with 10.5% oxygen and 12% water (simulating steam injection). Initial NO_x at 68 ppm corresponding to 0.5 gpm NO_x.

6.0 Modeling Results

Prior to this study Chemkin has been used to model RAPRENOx chemistry for use in Diesel applications. In an effort to model both the nitrogen and alkali metal reactions a collaborative effort was initiated with Dr. Jim Miller at Sandia National Labs. This effort was comprised of three parts; 1) an effort to develop a reaction set for NaOH chemistry that incorporated the latest thermochemistry and reaction set data for NaOH to explain the effect of NaOH chemistry on N_2O reduction 2) to improve the nitrogen chemistry model to explain past experimental results and to extend the verified model to gas turbine conditions and 3) to model the complete reaction set of nitrogen chemistry and NaOH chemistry to understand better the synergistic nature of NaOH and HNCO chemistry. This model is limited to the use of CO or H_2 as a fuel additive making

comparison to practical applications somewhat limited. We are able to predict the effects of temperature, fuel, O_2 concentration and N_2O concentration using this model. In addition, we are able to predict the effects of using NaOH in conjunction with HNCO.

The calculations are performed using SENKIN (2) in conjunction with CHEMKIN-II (3). The thermodynamic data come primarily from the CHEMKIN thermodynamic database (4), with a few additions and modifications. Table VI lists enthalpies and entropies for some potentially important species, and Appendix A lists the rate parameters for the reaction mechanism used in our calculations. The key points are discussed below.

Table VI. Thermodynamic Properties

Species	Hfo(298K) (kcal/mole)	So(298K) (cal/mole-K)
NaOH	-47.2	54.6
NaO	20.0	54.6
NaO_2	-12.2	62.5
Na	25.7	36.7
HNCO	-28.2	57.0
NCO	31.5	54.1
NH	85.2	43.3
NO	21.6	50.3
HNO	23.8	52.7
N_2O	19.6	52.5
CO	-26.4	47.2
CO_2	-94.0	51.0
H_2O	-57.8	45.1
H	52.1	27.4
OH	9.3	43.9
O	59.5	38.4

Nitrogen Chemistry

The nitrogen chemistry of interest is primarily that associated with the RAPRENO$_x$ process (NO reduction by cyanuric acid injection). The mechanism (Appendix A) is derived from the published work of Miller and Bowman (5, 6). Subsequently, our knowledge of the chemical kinetics and thermochemistry underlying the process has improved considerably. Many of these improvements have been documented and their impact discussed in other work related to NO_x formation and control (5, 7, 8). Nevertheless, we wish to review the main features of the mechanism here.

When cyanuric acid or HNCO is injected into exhaust gases containing CO (or perhaps some other fuel), water, and excess oxygen, the HNCO is converted to nitrogen-containing radicals by reaction with the active chain carriers in the CO-oxidation process,

$HNCO + OH$	=	$NCO + H_2O$	(R108)
$HNCO + H$	=	$NH_2 + CO$	(R104)
	=	$NCO + H_2$	(-R96)
$HNCO + O$	=	$NH + CO_2$	(R110)
	=	$NCO + OH$	(R111)
	=	$HNO + CO$	(R109).

All these rate coefficients have now been established fairly reliably, either experimentally, theoretically, or both. For k108, the rate coefficient for reaction (R108), we have adopted the expression given by Tsang (30), which is based on the experimental results of Tully, et al. (9) with some non-Arrhenius temperature dependence introduced. We have eliminated from the mechanism the alternative channel, $HNCO + OH$ " $NH_2 + CO_2$. The latter reaction was introduced by Miller and Bowman (6) in order to produce more chain branching in the reaction scheme. The additional chain branching appears now not to be essential (7, 8), and the original isotope labeling experiments of Tully, et al. (9) clearly indicate that $NCO + H_2O$ are the main products and perhaps the only significant ones. Nevertheless, we agree with Glarborg, et al. (7) and Bowman (8) that a direct determination of the branching fraction of the $OH + HNCO$ reaction is an important missing element in the available kinetic database.

Miller and Melius (10) have analyzed the reaction between hydrogen atoms and HNCO in some detail. The rate expressions they derive are in excellent agreement with experiment for both k104 and k96. We adopt their rate expressions here. He, et al. (11) have similarly studied the reaction of oxygen atoms with HNCO. Their results show that the dominant channels are (R110) and (R111) and that (R109) is relatively unimportant. This is a significant departure from the Miller and Bowman model (6) in which reaction (R109) was an important reaction. We adopt the results of He, et al. in the present work and discuss their implications below.

The most important mechanistic development since the Miller and Bowman (6) work involves the reaction of NCO with NO,

$NCO + NO$	=	$N_2O + CO$	(R94)
	=	$CO_2 + N_2$.	(R95)

This two-channel reaction is the primary NO removal step in the RAPRENOx process, and reaction (R94) is responsible for the N_2O that is formed in the process under most conditions. The work of Atakan and Wolfrum (12) and Mertens, et al. (13) clearly establish that the total rate coefficient, k94 + k95, drops off with temperature much more rapidly than assumed by Miller and Bowman. In this investigation we use the rate expression given by Mertens, et al. (13), which is an accurate representation of their data, as well as those of Perry (14) and Atakan and Wolfrum (12). Perhaps even more important than the rate coefficient is the branching fraction, k94 / (k94 + k95). Miller and Bowman assumed that the only products were $N_2O + CO$. However, subsequent work (15) has shown that both channels occur and that (R95) is dominant, at least at room temperature. We have adopted the branching fraction given by Cooper, et al. (15) independent of temperature. Our rate coefficients, k94 and k95, are in reasonably good agreement with those determined theoretically by Lin, et al. (16).

In establishing nitrous oxide concentrations, N_2O destruction reactions are equally as important as those that form N_2O. In RAPRENO$_x$, N_2O may be destroyed by one of the following reactions:

$N_2O + M$	=	$N_2 + O + M$	(R121)
$N_2O + H$	=	$N_2 + OH$	(R119, R120)
$N_2O + O$	=	$NO + NO$	(R123)
	=	$N_2 + O_2$	(R122)
$N_2O + OH$	=	$N_2 + HO_2$.	(R118)

The most important N_2O-destruction reaction is thermal dissociation, (R121). Our value of k121 comes from the work of Johnson, et al (17). The reaction of nitrous oxide with hydrogen atoms is incorporated into the mechanism as two separate reactions, (R119) and (R120). Both k119 and k120 have Arrhenius forms, and the sum k119 + k120 replicates the strong non-Arrhenius temperature dependence (apparently due to tunneling at low temperature) observed by Marshall, et al. (18). Our rate parameters are the same as those given in Ref. (18). For k123 and k122, i.e. the $O + N_2O$ reaction, we use the rate expressions determined by Davidson, et al. (19) in their high-temperature shock-tube experiments. Their experiments are the first ones to distinguish between the two channels sufficiently to determine different activation energies for k122 and k123. The reaction between nitrous oxide and hydroxyl, (R118) $N_2O + OH$, $N_2 + HO_2$, has been problematic in the past. It is clear that the reaction must be relatively slow, but it has not been clear just how slow. Frequently, even with a relatively small rate coefficient, reaction (R118) would show up as an important N_2O removal step in modeling. However, recently G2 and BAC-MP4 calculations have shown that the potential energy barrier for (R118) lies in the range 38 - 40 kcal/male (39). This makes (R118) prohibitively slow. The rate expression given in Appendix A is nothing more than a crude estimate.

Under conditions where water is not in abundance, isocyanic acid reacts primarily with oxygen atoms (6), producing NH as well as NCO,

$HNCO + O$	=	$NH + CO_2$	(R110)
	=	$NCO + OH$.	(R111)

In such a situation both NO and N_2O concentrations depend strongly on the reactions of NH with NO,

$NH + NO$	=	$N_2O + H$	(R115, R116)
	=	$N_2 + OH$,	(R117)

and with molecular oxygen,

$NH + O_2$	=	$NO + OH$	(R114)
	=	$HNO + O$.	(R113)

Miller and Melius (20) have analyzed these reactions in some detail, and we adopt their recommendations here.

Sodium Chemistry

The kinetics of elementary reactions involving alkali metals is a research area not nearly so well studied as the nitrogen chemistry described in the previous paragraphs. However, at least for

sodium, there appears to be enough information available for us to piece together a satisfactory kinetic model. Much of this chemistry has been reviewed recently by Plane (21).

The key reaction is that between sodium atoms and nitrous oxide,

$$Na + N_2O = N_2 + NaO. \qquad (R189)$$

The rate coefficient k189 has been measured several times (see (22) and references cited therein) with a remarkable degree of consistency among the results. Thus k189 appears to be known accurately up to T = 1000K. In our model we use the rate expression given by Plane and Rajasekhar (22).

Under virtually all conditions of interest, the most important reaction that competes with (R189) for the sodium atom is the addition reaction,

$$Na + O_2 + M = NaO_2 + M. \qquad (R198)$$

For our modeling we have adopted the rate coefficient for this reaction determined by Plane and Rajasekhar (22). Their experiments cover a wide temperature range, 233K < T < 1118K, and their results are in good agreement with other direct measurements (23-25) at common temperatures.

A key parameter in our modeling is the heat of formation of sodium superoxide, NaO_2. The value given in Table I is based on a Na-O_2 bond energy Do of 37.2 kcal/mole, which was determined theoretically by Partridge, et al. (26) and is believed to be accurate to within 2 kcal/mole. This value conflicts badly with recent values of Do(Na-O_2) derived from experiments, which give values of approximately 55 - 58 kcal/mole (27, 25). In our initial attempts at modeling N_2O reduction by sodium hydroxide, we used a kinetic model based on this higher value of Do(Na-O_2). However, with this large value of the bond energy NaO_2 became the most thermodynamically stable form the sodium could take, and our calculations indicated that all the NaOH was converted to NaO_2 during the N_2O removal process. This did not agree either with our chemical intuition or with these experimental observations which indicate that NaOH is the favored chemical form of sodium. The smaller value of Do(Na-O_2) resulted in calculations in which the initial and final concentrations of NaOH were essentially the same, as we expected. We thus adopted the low value of Do(Na-O_2) = 37.2 kcal/mole.

The rate coefficients for several reactions of NaO important to the present study have been measured in the last ten years (28, 29, 30, 21). These include

$$NaO + H_2O = NaOH + OH, \qquad (R190)$$
$$NaO + O = Na + O_2, \qquad (R191)$$
$$NaO + NO = Na + NO_2, \qquad (R194)$$
$$NaO + H_2 = NaOH + H, \qquad (R195)$$
and $$NaO + H_2 = Na + H_2O. \qquad (R196)$$

We have incorporated these results into our model. Other rate coefficients given in Appendix A are estimates. Nevertheless, we believe that the resulting kinetic model is sufficiently accurate to explore the possibility of using sodium hydroxide as a nitrous oxide removal agent.

6.1 Sodium Hydroxide Reduction of N_2O:

In this section we discuss the feasibility of using a fuel, such as hydrogen or carbon monoxide, to promote the conversion of NaOH to atomic sodium.

Hydrogen Addition

Figure 9 shows the effect of the addition of hydrogen to an exhaust stream derived from fuel-lean methane/air combustion where the exhaust contains 200 ppm nitrous oxide and 25 ppm NaOH. When fuel is added to this exhaust stream a major reduction in the nitrous oxide occurs, the exact amount of which depends on the quantity of fuel added. In Fig. 10 the same exhaust stream is subjected to varying amounts of NaOH addition along with 1% hydrogen fuel. It is clear that at higher NaOH levels even greater reduction in N_2O is possible.

While the exact free radical reaction scheme that generates the free Na depends on the exhaust composition and temperature, the following reaction chain summarizes the most important series of reactions that "catalytically" reduces N_2O in the presence of alkali metals (Na) and fuel (H_2):

	$H_2 + OH$	=	$H + H_2O$	(R1)
	$NaOH + H$	=	$Na + H_2O$	(R199)
	$Na + N_2O$	=	$NaO + N_2$	(R189)
	$NaO + H_2O$	=	$NaOH + OH$	(R190)
NET	$N_2O + H_2$	=	$H_2O + N_2$	

An important aspect of the use of NaOH to reduce N_2O is the strong dependence of sodium atom formation on the atomic hydrogen concentration. Since reaction (R199) is primarily responsible for producing the free sodium, reactions that limit the production of H atoms affect the conversion of NaOH to free sodium. Thus, the low-temperature limit for the effectiveness of the alkali metal chemistry is determined by the familiar competition between

	$H + O_2 = OH + O$	(9)
and	$H + O_2 + M = HO_2 + M.$	(R4, R5)

Because the Na-atom concentration follows the H-atom concentration, when the initial temperature is too low, the thermolecular reaction (R4, R5) dominates and not enough H atoms are produced by subsequent reactions of O and OH with fuel (or water) to produce the necessary Na atoms.

Once the free sodium atoms are formed, the dominant reaction that competes with reaction (R189) for the sodium is the thermolecular reaction

$$Na + O_2 + M = NaO_2 + M. \qquad (R198).$$

This reaction is the dominant Na removal step over virtually all conditions of interest, but its most important effects are seen at lower temperatures. The reaction tends to equilibrate very rapidly and this equilibration is what allows (R189) to compete and destroy the N_2O. Note that the extent to which (R198) can proceed in the forward direction before it equilibrates depends strongly on the heat of formation of NaO_2. The decrease in the effectiveness of NaOH in removing N_2O as the temperature is raised from 950K to 1050K, seen in Figs. 9 and 10, is due to radical reactions with NaO_2 that provide a pathway for recycling NaO_2 to NaOH.

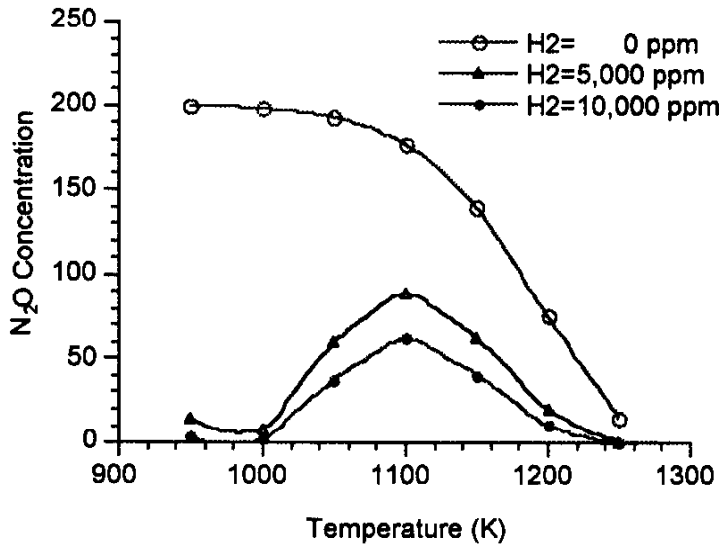

Figure 9: Calculated final N_2O concentration resulting from the addition of indicated NaOH concentration to a simulated exhaust stream containing 5% O_2, 16% H_2O, 8% CO_2, 200 ppm N_2O 1% H_2, and balance N_2. Final N_2O concentration is plotted for a reaction time of 1 second at all temperatures.

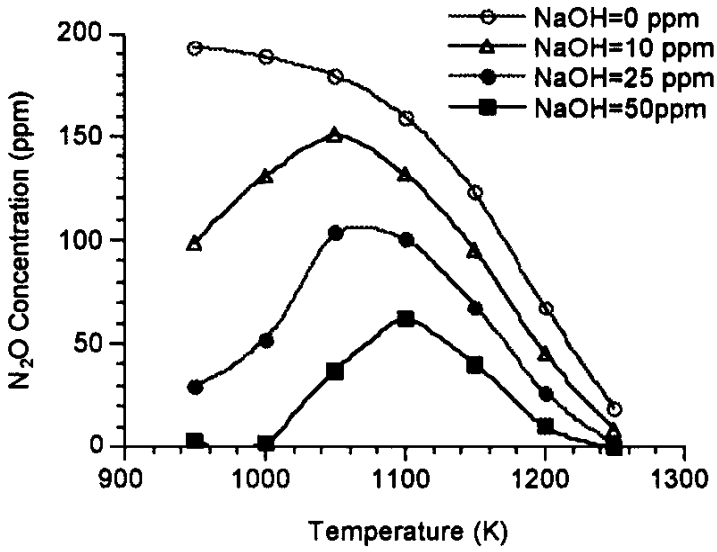

Figure 10. Calculated final N_2O concentration resulting from the addition of 0.0%, 0.5%, or 1% hydrogen addition to a simulated exhaust stream containing 5% O_2, 16% H_2O, 8% CO_2, 200 ppm N_2O, 50 ppm NaOH, and balance N_2. Final N_2O concentration is plotted for a reaction time of 1 second at all temperatures.

As the temperature is increased, reaction (-R2) increasingly dominates over (R4, R5), resulting in increased radical concentrations. These free radicals, particularly H-atoms, then react with NaO_2 and thus relieve the equilibration of reaction (R198) by recycling NaO_2 back to NaOH. The result is a less effective N_2O removal process as the temperature is increased. When our estimates of the rate coefficients for reactions

$$NaO_2 + H = NaOH + O \qquad (R207)$$

and

$$NaO_2 + H = NaO + OH \qquad (R204)$$

are reduced by two orders of magnitude from those listed in Appendix A, a somewhat improved N_2O reduction efficiency is obtained although the general trend remains the same.

The effect of molecular oxygen on the catalytic efficiency of atomic sodium is best illustrated in Fig. 11. A reduction in the amount of molecular oxygen in the exhaust (factor of 2) produces major improvement in N_2O reduction. This improvement in N_2O reduction efficiency is most evident at 950K and 1000K, where the N_2O concentrations are reduced to less than 5 ppm by the addition of 25 ppm NaOH to an exhaust with a composition of 2.5% oxygen and 200 ppm N_2O. Because reaction (R198) and subsequent reactions of NaO_2 with radical species play a determining role in the ability of atomic sodium to remove nitrous oxide from combustion exhaust streams, further investigation of these reactions, as well as of the heat of formation of NaO_2, is warranted.

Carbon Monoxide Addition

When carbon monoxide is chosen as the fuel supplement, rather than hydrogen, results such as those observed in Fig. 12 are obtained.
In addition to the generation of hydrogen atoms from reaction (R37), $OH + CO = CO_2 + H$, the direct reaction,

$$N_2O + CO = CO_2 + N_2, \qquad (R124)$$

contributes to the reduction of nitrous oxide at temperatures below 1050K. Note that this reaction occurs even without the addition of NaOH. The additional enhancement resulting from NaOH, as seen in Fig. 12, is not so dramatic as that from the addition of an equivalent amount of hydrogen. This is due to a competition for the CO between reaction (R124), which does not produce free radicals, and reaction (R37), which results in the production of hydrogen atoms. Note that reaction (R124) has a deleterious effect on N_2O removal when NaOH is added even though the reaction converts N_2O to N_2 directly.

At 950K reaction (R124) dominates reaction (R37) and limits CO-oxidation reactions that would otherwise produce H atoms. As the temperature is increased reaction (R37) become more important and Na atom production becomes more effective. Still the effectiveness of the process is limited by the ability of CO to produce hydrogen atoms. As the concentration of NaOH is increased, only a marginal reduction in the final N_2O concentration occurs.

Comparison with Experimental Results for RAPRENOx

In order to assess the accuracy of our kinetic model for the nitrogen chemistry, we compare our model predictions with the experimental results of Caton and Siebers (31, 32) for injection of cyanuric acid into simulated exhaust products. In order to make this comparison, we assume as has done before (6, 8,33,34) that the cyanuric acid powder instantaneously sublimes and decomposes into isocyanic acid when it is injected into the hot gas stream, i.e.

$$(HOCN)_3 \quad = \quad 3\ HNCO.$$

This assumption may lead to some inaccuracies, particularly at the lower end of the temperature range (6, 33) but for the present the assumption is necessary.

The comparisons are shown in Figures 13-16. The level of agreement between model and experiment is greatly improved over that obtained by Miller and Bowman (6), and it is approximately the same as that presented by Glarborg, et al. (7) and Bowman (8). The mechanism of the process remains essentially the same as that described in some detail by Miller and Bowman (6); the improved agreement between model and experiment is a direct result of improved knowledge of the rate coefficients and product distributions of the elementary reactions involved, not a drastic change in mechanism.

There are two mechanistic differences between the present model and that of Miller and Bowman that are worthy of note. The first involves case 3 of the Caton-Siebers data, i.e. the case in which no H_2O is present initially. For this case NO_f / NO_i at its minimum is substantially larger experimentally than for cases 1 and 2. The factor that distinguishes the present predictions from those of Miller and Bowman is the difference in the product distribution of the O + HNCO reaction. In the Miller-Bowman model, reaction (R109),

$$O + HNCO = HNO + CO, \qquad (R109)$$

is a major channel and leads directly to NO formation through HNO dissociation or reaction of HNO with OH,

$$HNO + OH = NO + H_2O, \qquad (R152)$$

thus resulting in a larger value of (NO_f/NO_i)min. In the present model (R109) does not occur appreciably and is replaced by

$$O + HNCO = NCO + OH \qquad (R111)$$

and

$$O + HNCO = NH + CO_2. \qquad (R110)$$

The value of (NO_f/NO_i)min predicted by the present mechanism is not so large as in the experiments or the Miller-Bowman model, but it appears to occur at approximately the same temperature as in the experiments. In the present model there is a very sensitive competition not only between NCO + NO and NCO + O (and O_2), but also between NH + NO and NH + O_2, resulting in a very narrow minimum. A minor adjustment in any one of these rate coefficients could lead to a larger value for (NO_f/NO_i)min. However, it is also possible that, if the minimum really occurs at T= 1300K (instead of T = 1275K as in the model), the experiments may have missed the minimum altogether.

The second difference between the present model and that of Miller and Bowman that we want to mention involves case 4 of the Caton-Siebers data, the case with no oxygen present initially. In the Miller-Bowman model, a major source of radicals for this case is the sequence

$NCO + NO$	=	$N_2O + CO$	(R94)
$N_2O + M$	=	$N_2 + O + M$	(R121)
$O + H_2O$	=	$OH + OH.$	(-R11)

The hydroxyl formed in (-R11) then reacts with HNCO to produce more NCO and thus sustain the process. In the present model (R94) is replaced by the two-channel reaction

$NCO + NO$	=	$N_2O + CO$	(R94)
$NCO + NO$	=	$N_2 + CO_2.$	(R95)

Not only is the total rate coefficient for the reaction smaller in the present model than in that of Miller and Bowman, but the primary products ($N_2 + CO_2$) are chain terminating, thus slowing the overall process down substantially. The origin of the discrepancy between model and experiment shown in Figure 16 is not obvious. However, molecular oxygen is always present in practical applications, so we shall not dwell on this point here.

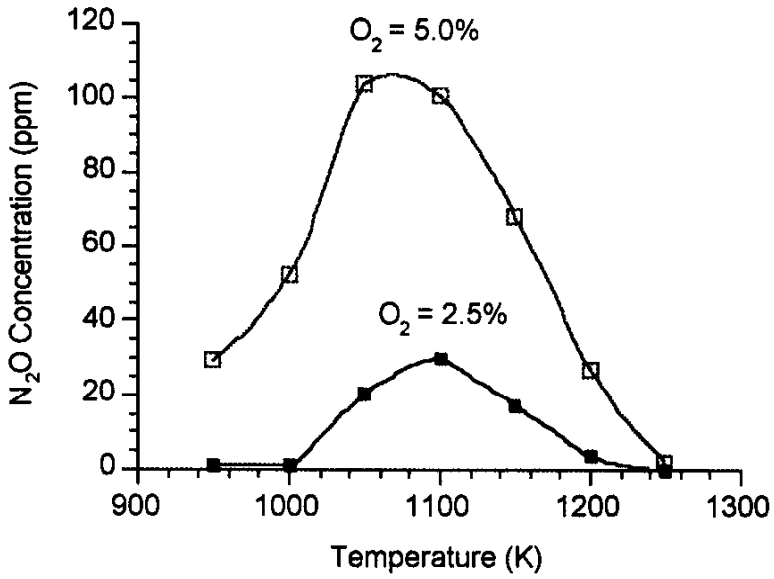

Figure 11. Calculated final N_2O concentration at 1 second residence time resulting from the addition of 25 ppm NaOH to an exhaust stream with the indicated O_2 concentration. Initial concentrations of other species are 10,000 ppm H_2, 16% H_2O, 8% CO_2, 200 ppm N_2O, and balance N_2

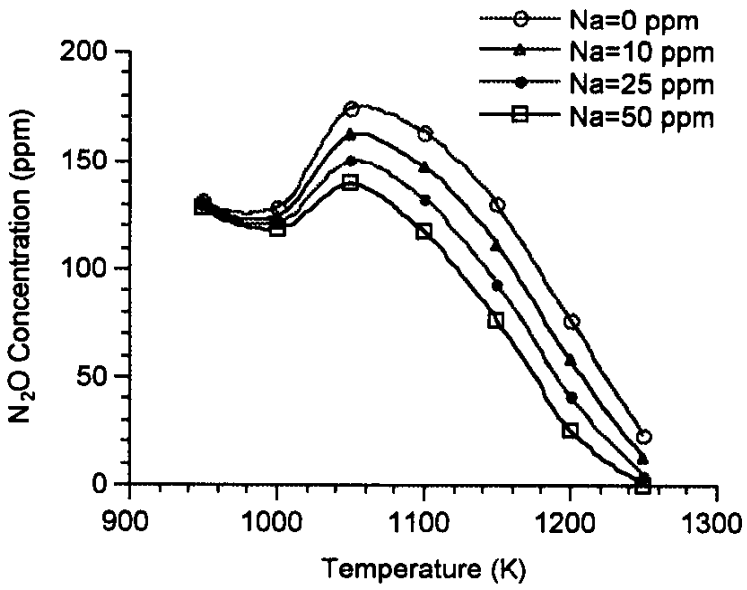

Figure 12. Calculated final N_2O concentration at 1 second for indicated NaOH concentrations in an exhaust containing 5,000 ppm CO, 5% O_2, compared with 16% H_2O, 8% CO_2, 200 ppm N_2O, and balance N_2.

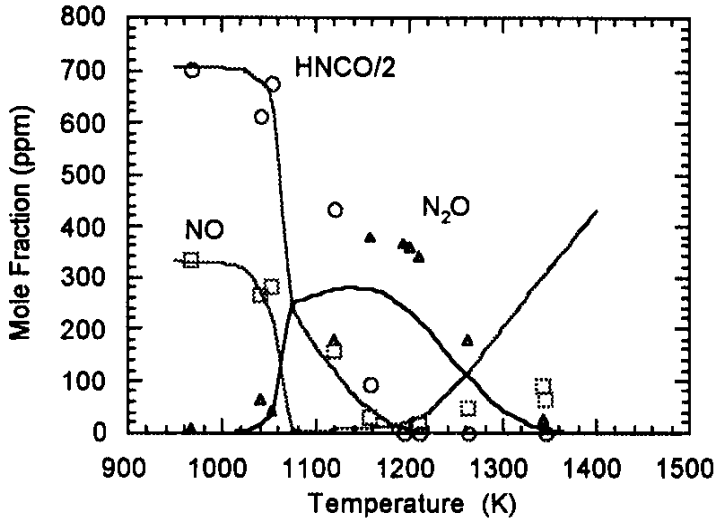

Figure 13. Plot of experimental data of Caton and Siebers (31,32) versus model predictions. Initial conditions: NO = 330 ppm; HNCO = 1410 ppm; CO = 1260 ppm; H_2O = 4.5%;O_2 = 12.3%; balance N_2; residence time = 867/T(K) s

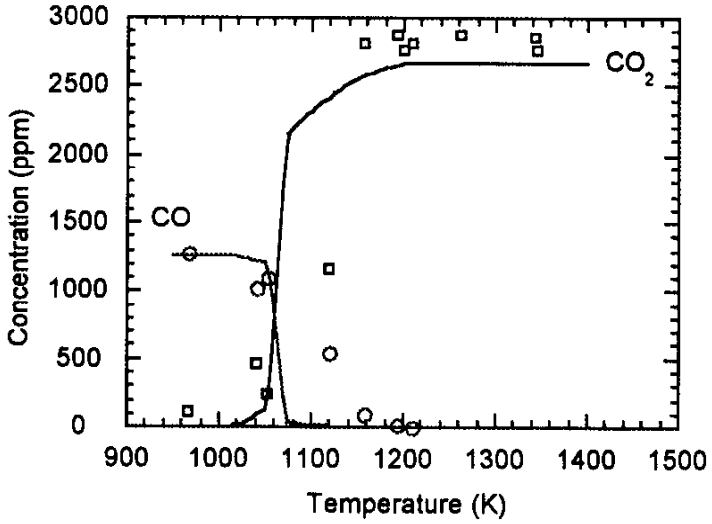

Figure 14. Plot of CO and CO_2 experimental data of Caton and Siebers (31,32) versus model calculations. Initial conditions: NO = 330 ppm; HNCO = 1410 ppm; CO = 1260 ppm; H_2O = 4.5%; O_2 - 12.3%; balance N_2 ; residence time = 867/T(K) s.

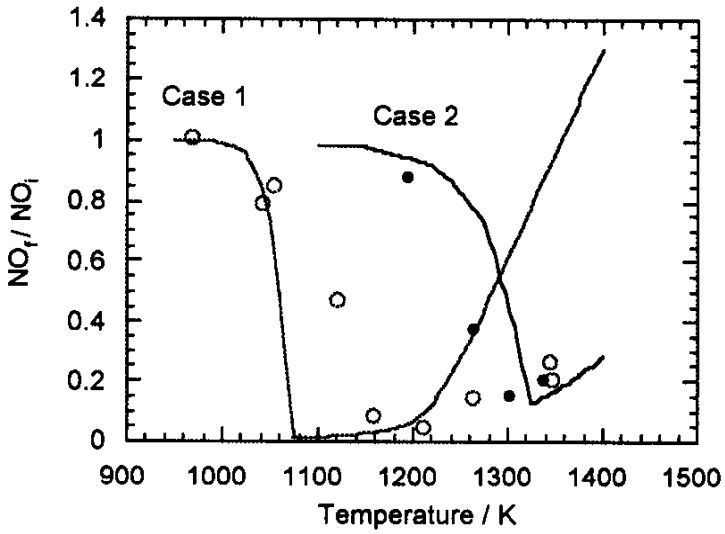

Figure 15. Plot of Case 1 (open circles) and Case 2 (filled circles) of Caton and Siebers (31,32):
Case 1 initial conditions: Same as Fig. 13.
Case 2 initial conditions: Same as Fig. 13 except that initial CO = 0

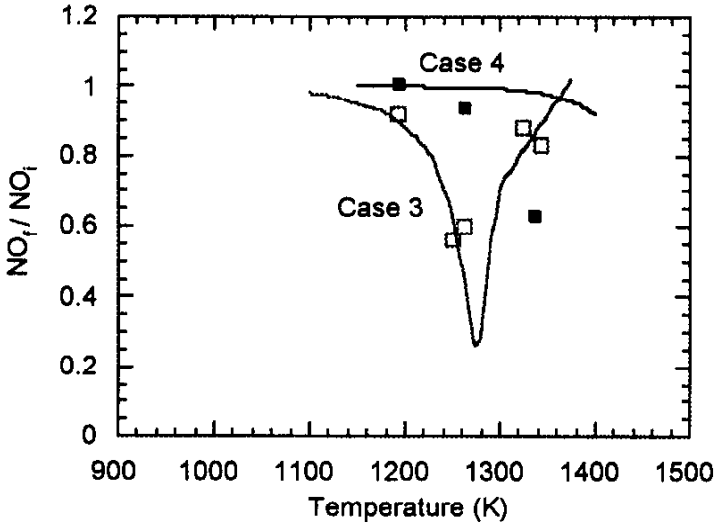

Figure 16. Plot of Case 3 (open squares) and Case 4 (filled squares) of Caton and Siebers (31,32) versus model calculations (solid line):

Case 3 initial conditions: Same as Fig. 13 except that initial $H_2O = 0$

Case 4 initial conditions: Same as Fig. 13 except that initial $O_2 = 0$

6.2 RAPRENOx Modeling with NaOH Chemistry Added:

Co-injection of NaOH with HNCO

One of the primary objectives of this study is to develop a technique for reducing unwanted nitrous oxide as a by-product from the use of RAPRENOx in NO_x reduction schemes. We have calculated the effect of using a fuel additive to promote nitrous oxide reduction using NaOH, and we have also shown that we can reasonably explain the experimental results of Caton and Siebers, especially the effects of CO on the efficiency of NO reduction by HNCO. Our next concern is to investigate the possibility of using a mixture of NaOH and HNCO to reduce NO without the production of nitrous oxide. To this end we have computed the emissions from a theoretical exhaust mixture containing 200 ppm NO, 300 ppm HNCO, 5% oxygen, 16% H_2O, 8% CO_2 and either 1,000 ppm H_2, 5,000 ppm H_2 or 5,000 ppm CO. Figs. 17 and 18 show the effects of adding of NaOH with 1,000 ppm hydrogen to this mixture. Note that at lower temperatures there is no effect of the addition of NaOH on the efficiency of the RAPRENOx process, i.e. with or without NaOH the NO_x levels are the same. Moreover, Fig. 17 demonstrates the ability of NaOH to improve the RAPRENOx efficiency at higher temperatures by reducing the peak radical concentrations. It does so by interfering with radical chain branching at these temperatures.

The addition of NaOH has the effect of shifting the temperature window to higher temperatures by about 50K and of widening the window slightly. This effect is associated with the ability of NaOH to promote the recombination of radicals thus limiting their concentrations.

While the effect on RAPRENOx is limited to the effect on the temperature window just described, the effect on the amount of nitrous oxide resulting from the process is seen in Fig. 18. Fifty ppm NaOH reduces the peak N_2O concentration by approximately a factor of two. Figures 19 and 20 show the effect of increasing the H_2 level to 5000 ppm on the same mixtures as Figs. 17 and 18. In Fig. 18 a very complex relationship is seen to exist between the NaOH chemistry and the RAPRENOx chemistry. The effect of NaOH on radical production completely obscures the effective window at 950K. At higher temperatures, once again the effect of NaOH on peak radical concentrations results in improved reduction of NOx.

When 5000 ppm CO are added to the exhaust stream with NaOH, a similar effect on the RAPRENO$_x$ process is observed as when hydrogen is added.(Figs. 21,22) The window is widened and the minimum is not so deep; i.e. less effective process. However, what is perhaps more interesting is that the N_2O reduction efficiency is less pronounced than when H_2 is added, although the general trends are the same.

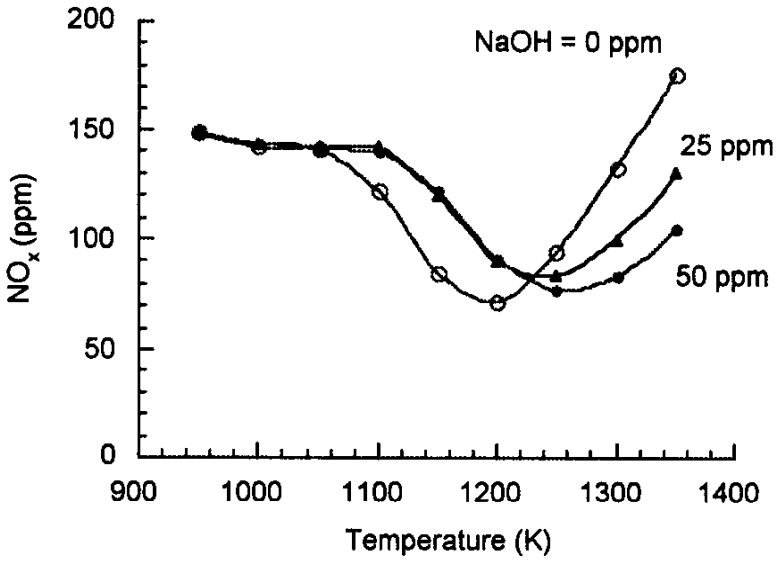

Figure 17. Plot of calculated effect of 0, 25, or 50 ppm NaOH on a simulated exhaust gas mixture. Initial conditions: NO = 200 ppm; HNCO = 300 ppm; H_2 = 1,000 ppm; O_2 = 5%; CO_2 = 8%; H_2O = 16%; balance N_2. Residence time = 1 s.

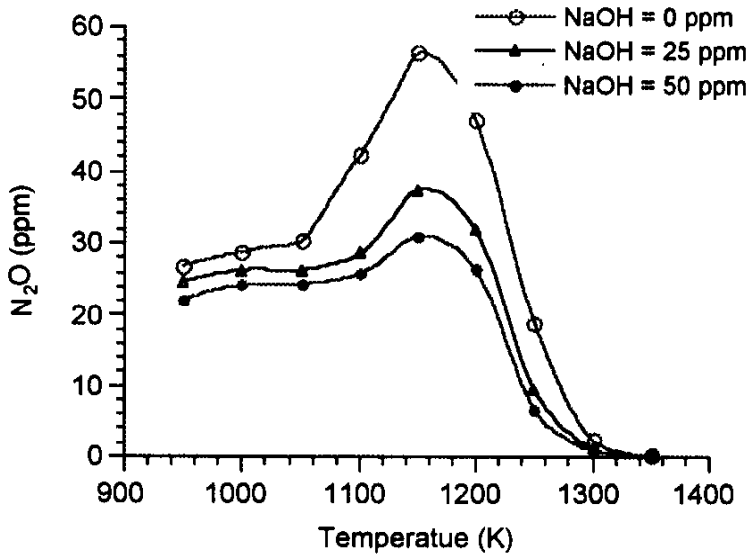

Figure 18. Plot of nitrous oxide concentration resulting from the effect of 0, 25, or 50 ppm NaOH on a simulated exhaust gas mixture. Initial conditions: NO = 200 ppm; HNCO = 300 ppm; H_2 = 1,000 ppm; O_2 = 5%; CO_2 = 8%; H_2O = 16%; balance N_2. Residence time = 1 s.

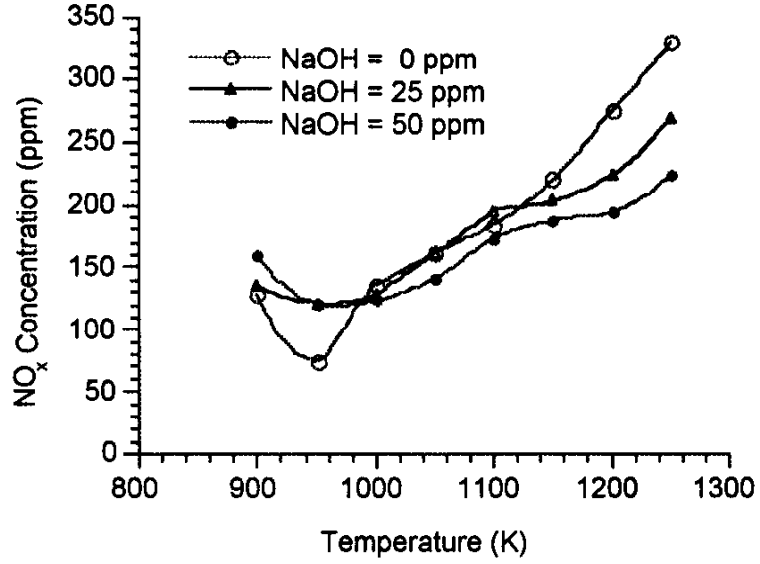

Figure 19. Plot of calculated effect of 0, 25, or 50 ppm NaOH on a simulated exhaust gas mixture. Initial conditions: NO = 200 ppm; HNCO = 300 ppm; O_2 = 5%; H_2 = 5,000 ppm; CO_2 = 8%; H_2O = 16%; balance N_2. Residence time = 1 s

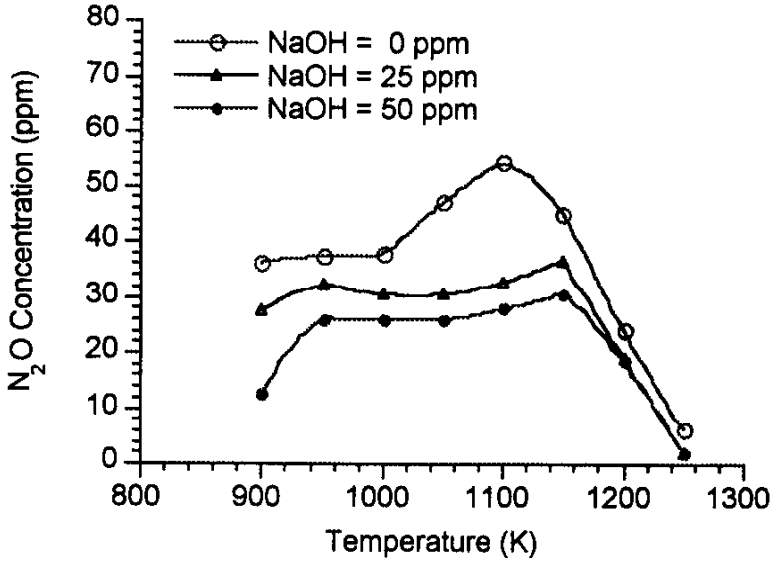

Figure 20. Plot of nitrous oxide concentration resulting from effect of 25 or 50 ppm NaOH on a simulated exhaust gas mixture. Initial conditions: NO = 200 ppm; HNCO = 300 ppm; H_2 = 5,000 ppm; O_2 = 5%; CO_2 = 8%; H_2O = 16%; balance N_2. Residence time = 1 s.

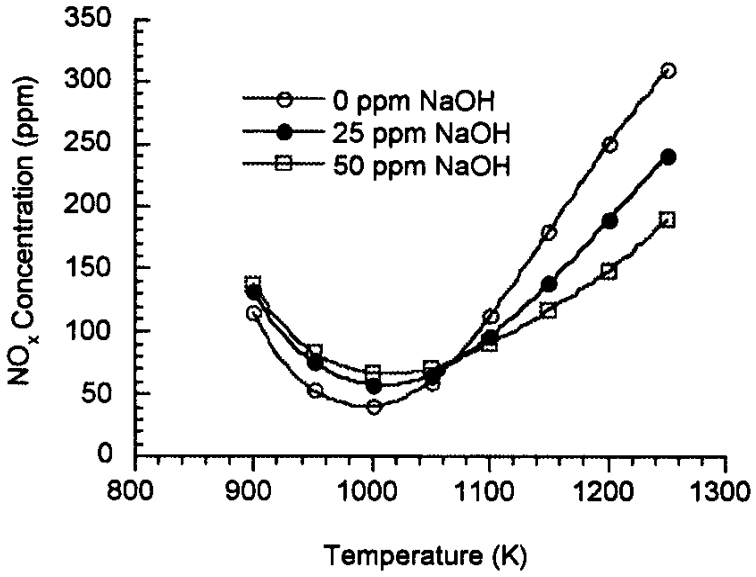

Figure 21. Plot of calculated effect of 25 or 50 ppm NaOH on a simulated exhaust gas mixture. Initial conditions: NO = 200 ppm; HNCO = 300 ppm; CO = 5,000 ppm; O_2 = 5%; CO_2 = 8%; H_2O = 16%; balance N_2. Residence time = 1 s.

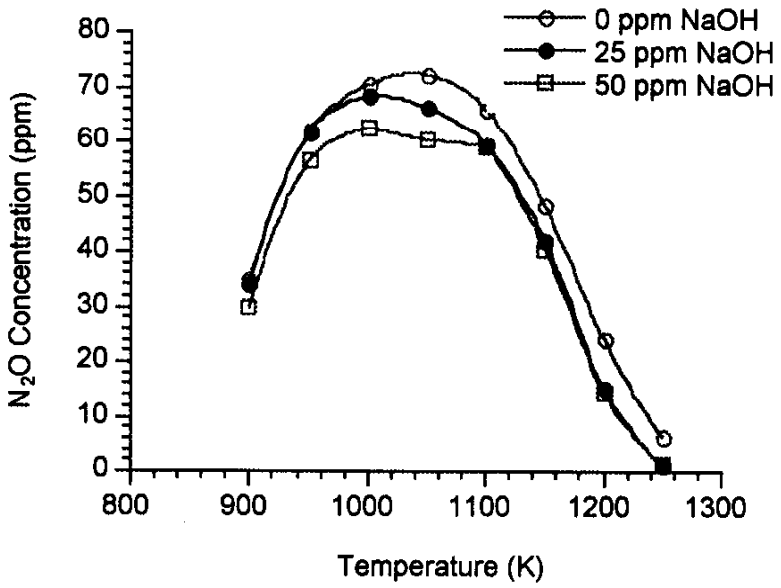

Figure 22. Plot of nitrous oxide concentration resulting from effect of 0, 25, or 50 ppm NaOH on a simulated exhaust gas mixture. Initial conditions: NO = 200 ppm; HNCO = 300 ppm; CO = 5,000 ppm; O_2 = 5%; CO_2 = 8%; H_2O = 16%; balance N_2. Residence time = 1 s.

Model Summary and Conclusions

As a representative alkali-metal compound, we have investigated the use of sodium hydroxide to control nitrous oxide emissions from combustion sources. The key elementary reaction is

$$Na + N_2O = N_2 + NaO. \qquad (R189)$$

Reaction (R189) is relatively fast (as are the reactions of other alkali-metal atoms with N_2O). Free sodium atoms are produced by the reaction,

$$H + NaOH = Na + H_2O, \qquad (R199)$$

when small quantities of fuel are added with the sodium hydroxide. The cycle is completed by the reaction,

$$NaO + H_2O = NaOH + OH. \qquad (R190)$$

As a consequence of this recycling of the sodium atom back to NaOH, one sodium atom is potentially capable of removing a large number of N_2O molecules, thus producing a very efficient process.

Even though reaction (R189) is fast it is allowed to occur only to the extent that the faster reaction,

$$Na + O_2 + M = \quad NaO_2 + M, \qquad (R198)$$

equilibrates. At sufficiently high temperatures this equilibration can be disturbed by the reaction of free radicals with NaO_2, i.e. when radical attack on NaO_2 begins to compete with the reverse of reaction (R198). The competition between reactions (R189) and (R198) and the equilibration of reaction (R198) make our predictions sensitive not only to the values of k189 and k198, but also to the Na-O_2 bond energy. The very large discrepancy of approximately 20 kcal/mole between experimental and theoretical values of this latter quantity clearly needs to be resolved.

While it is difficult to extrapolate our calculations directly to practical applications where a wide variety of exhaust conditions may exist, the present results suggest practical steps to be made in the application of alkali metals to the reduction of nitrous oxide. First, sufficient hydrogen atoms should be present, through the addition of small amounts of fuel or by the injection of NaOH into the combustion chamber or reburn section of a staged combustor. Secondly, alkali metals may reduce nitrous oxide production from selective non-catalytic processes such as from RAPRENOx, but it is best to add an additional region for this purpose, following the actual application of the SNCR process to provide the maximum NO_x reduction and the maximum N_2O removal.

One further result from this study is the prediction that alkali metals will have an effect on the efficiency of the RAPRENO$_x$ process. Alkali metals broaden the temperature window and impact the efficiency of the process in a complex manner, sometimes reducing NO_x, particularly at higher temperatures or in reducing efficiency at minimum of NO_f/NO_i.

7.0 TECHNICAL SUMMARY FOR GAS TURBINE APPLICATIONS:

Based upon the experimental effort the technical requirements that are needed to reduce NOx in a gas turbine location are 1) a reaction vessel that provides a chamber for the reaction chemistry to reach completion, 2) sufficient fuel injection to raise the temperature to approximately 725 C and, a molar ratio of HNCO to NO_x determined by the initial concentration of NO_x varying from 1.2-4.0/1. Under these conditions it is possible to reach very high NO_x reduction. The following considerations are discussed in more detail.

Reaction Chamber

The reaction chamber should be constructed of mild steel with a high temperature liner and it should be constructed to minimize surface to volume ratio while providing for gas flow recirculation to stabilize the chemistry. While it is possible to use a flat plate to stabilize the reaction zone, evident by lower CO concentration, the use of a flat plate does not insure the most efficient utilization of cyanuric acid perhaps due to temperature gradients in the reactor. The reaction chamber should provide a 1 second residence time for reaction in order to minimize the necessary consumption of cyanuric acid and obtain the best efficiency.

Fuel Injection

The use of fuel to raise the temperature and enhance the radical generation ability places some major constraints on operation of RAPRENOx. This is due to the additional cost of operation associated with increase fuel usage. While this additional cost may be mitigated by using the additional heat to generate steam or by providing low value heat for other co-gen uses, in the case where no additional use for the heat exists a heat exchanger must be used to minimize fuel consumption. Based upon the results of these experiments we would require 10-20% additional fuel to raise the temperature of typical exhaust from an Allison 501-Ka gas turbine.

With these limitations and requirements it is possible to significantly reduce nitric oxide in an exhaust system derived from a gas turbine. The use of alkali metals to reduce any nitrous oxide produced appears to be a possible approach for minimizing nitrous oxide derived as a byproduct from the RAPRENOx process if so required.

8.0 REFERENCES:

1. R. A. Perry, First International Conference on Combustion Technologies for a Clean Environment, presented, Vilamoura, Portugal (1991)
2. A. E. Lutz, R. J. Kee, and J. A. Miller, "SENKIN: A Fortran Program for Predicting Homogenous Gas Phase Chemical Kinetics with Sensitivity Analysis," Sandia National Laboratories Report SAND87-8248 (1988)
3. R. J. Kee, F. M. Rupley, and J. A. Miller, "CHEMKIN-II, A Fortran Chemical Kinetics Package for the Analysis of Gas-Phase Chemical Kinetics," Sandia National Laboratories Report SAND87-8215B (1989)
4. R. J. Kee, F. M. Rupley, and J. A. Miller, "The CHEMKIN Thermodynamic Data Base," Sandia National Laboratories Report SAND87-8215B (1990)
5. J. A. Miller and C. T. Bowman, Prog. Energy Combust. Sci. 15, 287 (1989)
6. J. A. Miller and C. T. Bowman, Int. J. Chem. Kin.. 23, 289 (1991).
7. P. Glarborg, P. G. Kristenson, S. H. Jensen, and K. Dam-Johansen, Combust. Flame (in press)
8. C. T. Bowman, "Mechanisms and Modeling of Gas-Phase Aftertreatment Methods for NO Removal from Combustion Products" Comb. Sci. Technology, in press (1995)
9. F. P. Tully, R. A. Perry, L. R. Thorne, and M. D. Allendorf, Twenty-Second Symposium (International) on Combustion, The Combustion Institute, p. 1101 (1989)
10. J. A. Miller and C. F. Melius, Int. J. Chem. Kin. 24, 421 (1992)
11. Y. He, M. C. Lin, C. H. Wu, and C. F. Melius, Twenty-Fourth Symposium (International) on Combustion, The Combustion Institute, P. 711 (1992)
12. B. Atakan and J. Wolfrum, Chem. Phys. Lett. 178, 157 (1991)
13. J. D. Mertens, A. J. Dean, R. K. Hanson, and C. T. Bowman, Twenty-Fourth Symposium (International) on Combustion, The Combustion Institute, p. 701 (1992)
14. R. A. Perry, J. Chem. Phys. 82, 5485 (1985)
15. W. F. Cooper and J. F. Hershberger, J. Phys. Chem. 96, 771 (1992)
16. M. C. Lin, Y. He, and C. F. Melius, J. Phys. Chem. 97, 9124 (1993)
17. J. E. Johnsson, P. Glarborg, and K. Dam-Johansen, Twenty-Fourth Symposium (International) on Combustion, The Combustion Institute, p. 917 (1992)
18. P. Marshall, A. Fontijn, and C. F. Melius, J. Chem. Phys. 86, 5540 (1987)
19. D. F. Davidson, M. D. DiRosa, A. Y. Chang, and R. K. Hanson, Proceedings of the 8th International Symposium on Shock Waves, Vol. 2, Springer-Verlag, p. 813 (1991)
20. J. A. Miller and C. F. Melius, Twenty-Fourth Symposium (International) on Combustion, The Combustion Institute, p. 719 (1992)
21. J. M. C. Plane , International Reviews in Phys. Chem. 10, 55-106 (1991).
22. J. M. C. Plane and B. Rajasekhar, J. Phys. Chem. 93, 3135 (1989).
23. J. A. Silver, M. S. Zahniser, A. C. Stanton, and C. E. Kolb, Twentieth Symposium (International) on Combustion, the Combustion Institute, p.605 (1984).
24. D. Husain, P. Marshall, and J. M. C. Plane, J. Chem. Soc. Faraday Trans. 281, 301 (1985).
25. P. Marshall, A. S. Narayan, and A. Fontijn, J. Phys. Chem. 94, 2998 (1990).
26. C. P. Fenimore and J. R. Kelso, J. Amer. Chem. Soc. 72, 5045 (1950).
27. K. Schofield and M. Steinberg , J . Phys. Chem. 96, 715 (1992).
28. J. M. C. Plane and D. Husain, J. Chem. Soc. Faraday Trans. 2 82, 2047 (1986)

29. J. W. Ager III, C. L. Talcott, and C. J. Howard, J. Chem. Phys. 85, 5584-5592 (1986).
30. J. W. Ager III and C. J. Howard, J. Chem. Phys., 87(2), 921 (1987).
31. J.A. Caton and D. L. Siebers, Comb. Sci. Tech. 65, 277 (1989).
32. D. L. Siebers and J. A. Caton, Comb. Flame 79, 31 (1990)
33. J. A. Miller and C. T. Bowman, Prog. Energy Combust. Sci. 15, 287 (1989).
34. P. Glarborg, P. G. Kristenson, S. H. Jensen, and K. Dam-Johansen, Combust. Flame
35. L. Ho, S. L. Chen, , W. R. Seeker, and P. M. Maly, U.S. patent #5,270,025, December 14, 1993.

Appendix A
(k = A T**b exp(-E/RT))

REACTIONS CONSIDERED	A	b	E
1. $OH+H_2=H_2O+H$	2.14E+08	1.5	3449
2. $O+OH=O_2+H$	2.02E+14	-.4	0
3. $O+H_2=OH+H$	5.06E+04	2.7	6290
4. $H+O_2+M=HO_2+M$	2.10E+18	-1.0	0
Enhanced third body efficiencies: $H_2O=10, CO_2=4.2, H_2=2.9$, CO=2			
5. $H+O_2+N_2=HO_2+N_2$	6.70E+19	-1.4	0
6. $OH+HO_2=H_2O+O_2$	2.89E+13	.0	-497
7. $H+HO_2=OH+OH$	1.69E+14	.0	874
8. $H+HO_2=H_2+O_2$	4.28E+13	.0	1411
9. $H+HO_2=O+H_2O$	3.01E+13	.0	1721
10. $O+HO_2=O_2+OH$	3.25E+13	.0	0
11. $2OH=O+H_2O$	4.33E+03	2.7	-2486
12. $H+H+M=H_2+M$	1.00E+18	-1.0	0
Enhanced third body efficiencies: $H_2O=H_2=CO_2=0$			
13. $H+H+H_2=H_2+H_2$	9.20E+16	-.6	0
14. $H+H+H_2O=H_2+H_2O$	6.00E+19	-1.3	0
15. $H+H+CO_2=H_2+CO_2$	5.49E+02	-2.0	0
16. $H+OH+M=H_2O+M$	1.60E+22	-2.0	0
Enhanced third body efficiencies: $H_2O=5$			
17. $H+O+M=OH+M$	6.20E+16	-.6	0
Enhanced third body efficiencies: $H_2O=5$			
18. $O+O+M=O_2+M$	1.89E+13	.0	-1788
Enhanced third body efficiencies: $H_2O=5$, $H_2=CO=2$, $CO_2=3$			
19. $HO_2+HO_2=H_2O_2+O_2$	4.20E+14	.0	11982
20. $HO_2+HO_2=H_2O_2+O_2$	1.30E+11	.0	-1629
21. $H_2O_2+M=OH+OH+M$	1.30E+17	.0	45500
Enhanced third body efficiencies: $H_2O=5$, $H_2=CO=2$, $CO_2=3$			
22. $H_2O_2+H=HO_2+H_2$	1.69E+12	.0	3755
23. $H_2O_2+H=OH+H_2$	1.02E+13	.0	3576
24. $H_2O_2+O=OH+HO_2$	6.63E+11	.0	3974
25. $H_2O_2+OH=H_2O+HO_2$	7.83E+12	.0	1331
26. $CH_2O+OH=HCO+H_2O$	3.43E+09	1.2	-447
27. $CH_2O+H=HCO+H_2$	2.19E+08	1.8	3000

28.	$CH_2O+M=HCO+H+M$	3.31E+16	.0	81000
	Enhanced third body efficiencies:			
	$H_2O=5$, $H_2=CO=2$, $CO_2=3$			
29.	$CH_2O+O=HCO+OH$	1.80E+13	.0	3080
30.	$HCO+OH=H_2O+CO$	1.00E+14	.0	0
31.	$HCO+M=H+CO+M$	1.86E+17	-1.0	17000
	Enhanced third body efficiencies:			
	$H_2O=5.0$, $H_2=1.9$, $CO=1.9$, $CO_2=3.0$			
32.	$HCO+H=CO+H_2$	1.19E+13	.3	0
33.	$HCO+O=CO+OH$	3.00E+13	.0	0
34.	$HCO+O=CO_2+H$	3.00E+00	.0	0
35.	$HCO+O_2=HO_2+CO$	3.30E+13	-.4	0
36.	$CO+O+M=CO_2+M$	6.17E+14	.0	3000
	Enhanced third body efficiencies:			
	$H_2O=5$, $H_2=CO=2$, $CO_2=3$			
37.	$CO+OH=CO_2+H$	1.51E+07	1.3	-758
38.	$CO+O_2=CO_2+O$	2.50E+12	.0	47688
39.	$CO+HO_2=CO_2+OH$	5.80E+13	.0	22934
40.	$CO_2+N=NO+CO$	1.90E+11	.0	3400
41.	$CN+H_2O=HCN+OH$	8.00E+12	.0	7450
42.	$HCN+OH=HOCN+H$	5.85E+04	2.4	12500
43.	$HCN+OH=HNCO+H$	1.98E-03	4.0	1000
44.	$HCN+OH=NH_2+CO$	7.83E-04	4.0	4000
45.	$HOCN+OH=NCO+H_2O$	6.38E+05	2.0	2563
46.	$HOCN+H=HNCO+H$	2.00E+07	2.0	2000
47.	$HOCN+O=NCO+OH$	1.50E+04	2.6	4000
48.	$HCN+O=NCO+H$	1.38E+04	2.6	4980
49.	$HCN+O=NH+CO$	3.45E+03	2.6	4980
50.	$HCN+O=CN+OH$	2.70E+09	1.6	29200
51.	$CN+H_2=HCN+H$	2.95E+05	2.5	2237
52.	$CN+O=CO+N$	7.70E+13	.0	0
53.	$CN+O_2=NCO+O$	7.47E+12	.0	0
54.	$CN+OH=NCO+H$	6.00E+13	.0	0
55.	$HCN+CN=C_2N_2+H$	1.32E+03	2.7	646
56.	$CN+NO_2=NCO+NO$	5.32E+15	-.8	344
57.	$CN+NO_2=CO+N_2O$	4.93E+14	-.8	344
58.	$CN+NO_2=CO_2+N_2$	3.70E+14	-.8	344
59.	$CN+N_2O=NCN+NO$	3.85E+03	2.6	3696
60.	$CN+CO_2=NCO+CO$	3.67E+06	2.2	26884
61.	$NO_2+NO_2=NO+NO+O_2$	1.63E+12	.0	26123
72.	$NO_2+NH=N_2O+OH$	1.00E+13	.0	0
73.	$NO_2+NH_2=N_2O+H_2O$	3.20E+18	-2.2	0
74.	$NO_2+NH_2=H_2NO+NO$	3.50E+12	.0	0
75.	$NO_2+HNO=HONO+NO$	6.00E+11	.0	2000
76.	$NO_2+H=NO+OH$	8.40E+13	.0	0

77	$NO_2+O=NO+O_2$	3.90E+12	.0	-238
78	$NO+O+M=NO_2+M$	7.50E+19	-1.4	0
	Enhanced third body efficiencies:			
	N_2=1.7, O_2=1.5, H_2O=10, H_2=2, CO=2, CO_2=3,			
79	$HONO+OH=H_2O+NO_2$	4.00E+12	0	0
80	$HONO+NH_2=NO_2+NH_3$	5.00E+12	0	0
81	$H_2NO+NO_2=HONO+HNO$	6.00E+11	0	2000
82	$NO_2+CO=CO_2+NO$	9.00E+13	0	33779
83	$OH+NO+M=HONO+M$	5.08E+23	-2.5	-68
	Enhanced third body efficiencies:			
	H_2O=5. H_2=2, CO=2, CO_2=0			
84	$OH+NO+CO_2=HONO+CO_2$	1.71E+23	-2.3	-246
85	$HONO+O=OH+NO_2$	1.20E+13	0	5961
86	$HONO+H=H_2+NO_2$	1.20E+13	0	7352
87	$HONO+HCO=NO_2+CH_2O$	1.20E+03	2.4	3855
88	$NCO+O_2=NO+CO_2$	2.00E+12	0	20000
89	$NCO+H=NH+CO$	5.00E+13	0	0
90	$NCO+O=NO+CO$	4.70E+13	0	0
91	$NCO+N=N_2+CO$	2.00E+13	0	0
92	$NCO+OH=NO+HCO$	5.00E+12	0	15000
93	$NCO+M=N+CO+M$	3.10E+16	-0.5	48000
	Enhanced third body efficiencies:			
	H_2O=5, H_2=CO=2, CO_2=3			
94	$NCO+NO=N_2O+CO$	6.16E+17	-1.7	763
95	$NCO+NO=N_2+CO_2$	7.84E+17	-1.7	763
96	$NCO+H_2=HNCO+H$	7.59E+02	3	4000
97	$NCO+NCO=N_2+2CO$	1.80E+13	0	0
98	$NCO+HNO=HNCO+NO$	1.80E+13	0	0
99	$NCO+HONO=HNCO+NO_2$	3.60E+12	0	0
100	$NCO+NO_2=CO+2NO$	2.50E+11	0	-707
101	$NCO+NO_2=CO_2+N_2O$	3.00E+12	0	-707
102	$NCO+HCO=HNCO+CO$	3.60E+13	0	0
103	$NCO+CH_2O=HNCO+HCO$	6.00E+12	0	0
104	$HNCO+H=NH_2+CO$	2.25E+07	1.7	3800
105	$HNCO+M=NH+CO$	1.14E+16	0	86000
	Enhanced third body efficiencies:			
	H_2O=5, H_2=CO=2, CO_2=3			
106	$HNCO+NH=NH_2+NCO$	3.00E+13	0	23700
107	$HNCO+NH_2=NH_3+NCO$	5.00E+12	0	6200
108	$OH+HNCO=NCO+H_2O$	6.38E+05	2	2563
109	$HNCO+O=HNO+CO$	1.49E+08	1.6	44012
110	$HNCO+O=NH+CO_2$	9.80E+07	1.4	8524
111	$HNCO+O=NCO+OH$	2.20E+06	2.1	11425
112	$HNCO+HO_2=NCO+H_2O_2$	3.00E+11	0	22000
113	$NH+O_2=HNO+O$	4.61E+05	2	6500

114	$NH+O_2=NO+OH$	1.28E+06	1.5	100
115	$NH+NO=N_2O+H$	2.94E+14	-0.4	0
116	$NH+NO=N_2O+H$	2.16E+13	-0.2	0
117	$NH+NO=N_2+OH$	2.16E+12	-0.2	0
118	$N_2O+OH=N_2+HO_2$	2.00E+12	0	40000
119	$N_2O+H=N_2+OH$	3.31E+10	0	4729
120	$N_2O+H=N_2+OH$	4.40E+14	0	19254
121	$N_2O+M=N_2+O+M$	4.00E+14	0	56100
	Enhanced third body efficiencies: N_2=1.6, O_2=CO=1.5, H_2O=10, CO_2=3			
122	$N_2O+O=N_2+O_2$	1.40E+12	0	10800
123	$N_2O+O=NO+NO$	2.90E+13	0	23150
124	$N_2O+CO=N_2+CO_2$	3.19E+11	0	20237
125	$NH+OH=HNO+H$	2.00E+13	0	0
126	$NH+OH=N+H_2O$	5.00E+11	0.5	2000
127	$NH+N=N_2+H$	3.00E+13	0	0
128	$NH+H=N+H_2$	3.00E+13	0	0
129	$NH+O=NO+H$	9.20E+13	0	0
130	$NH_2+O=HNO+H$	6.63E+14	-0.5	0
131	$NH_2+O=NH+OH$	6.75E+12	0	0
132	$NH_2+OH=NH+H_2O$	4.00E+06	2	1000
133	$NH_2+H=NH+H_2$	6.92E+13	0	3650
134	$NH_2+HO_2=NH_3+O_2$	1.00E+13	0	0
135	$NH_2+HO_2=H_2NO+OH$	5.00E+13	0	0
136	$NH_2+NO=NNH+OH$	2.80E+13	-0.6	0
137	$NH_2+NO=N_2+H_2O$	1.30E+16	-1.3	0
138	$NH_2+NO=N_2+H_2O$	2.80E+13	-0.6	0
139	$NH_3+OH=NH_2+H_2O$	2.04E+06	2	566
140	$NH_3+H=NH_2+H_2$	6.36E+05	2.4	10171
141	$NH_3+O=NH_2+OH$	2.10E+13	0	9000
142	$NH_3+HO_2=NH_2+H_2O_2$	3.00E+11	0	22000
143	$NNH=N_2+H$	1.00E+06	0	0
144	$NNH+NO=N_2+HNO$	5.00E+13	0	0
145	$NNH+H=N_2+H_2$	1.00E+14	0	0
146	$NNH+OH=N_2+H_2O$	5.00E+13	0	0
147	$NNH+NH_2=N_2+ NH_3$	5.00E+13	0	0
148	$NNH+NH=N_2+NH_2$	5.00E+13	0	0
149	$NNH+O=N_2O+H$	1.00E+14	0	0
150	$NNH+O=NH+NO$	5.00E+13	0	0
151	$HNO+M=H+NO+M$	1.50E+16	0	48680
	Enhanced third body efficiencies: H_2O=10, $O_2=N_2=H_2$=CO=2, CO_2=3			
152	$HNO+OH=NO+H_2O$	3.60E+13	0	0
153	$HNO+H=H_2+NO$	4.46E+11	0.7	655
154	$HNO+NH_2= NH_3+NO$	2.00E+13	0	1000

155	$HNO+HNO=N_2O+H_2O$ 3.95E+12	0	5000	
156	$HNO+NO=N_2O+OH$	2.00E+12	0	26000
157	$HNO+HCO=CH_2O+NO$	6.00E+11	0	2000
158	$HNO+O_2=HO_2+NO$	1.00E+13	0	25000
159	$H_2NO+O=NH_2+O_2$	4.00E+13	0	0
160	$H_2NO+M=HNO+H+M$	5.00E+16	0	50000
	Enhanced third body efficiencies: H_2O=5, N_2=H_2=CO=2, CO_2=3			
161	$H_2NO+H=HNO+H_2$	3.00E+07	2	2000
162	$H_2NO+H=NH_2+OH$	5.00E+13	0	0
163	$H_2NO+O=HNO+OH$	3.00E+07	2	2000
164	$H_2NO+OH=HNO+H_2O$ 2.00E+07	2	100	
165	$H_2NO+NO=HNO+HNO$	2.00E+07	2	13000
166	$H_2NO+NH_2= NH_3+HNO$	3.00E+12	0	1000
167	$N+NO=N_2+O$	3.27E+12	0.3	0
168	$N+O_2=NO+O$	6.40E+09	1	6280
169	$N+OH=NO+H$	3.80E+13	0	0
170	$NH_2+NH=N_2H_2+H$	5.00E+13	0	0
171	$NH+NH=N_2+H+H$	2.54E+13	0	0
172	$NH_2+N=N_2+H+H$	7.20E+13	0	0
173	$N_2H_2+M=NNH+H+M$	5.00E+16	0	50000
	Enhanced third body efficiencies: H_2O=15, O_2=N_2=H_2=CO=2, CO_2=3			
174	$N_2H_2+H=NNH+H_2$	5.00E+13	0	1000
175	$N_2H_2+O=NH_2+NO$	1.00E+13	0	0
176	$N_2H_2+O=NNH+OH$	2.00E+13	0	1000
177	$N_2H_2+OH=NNH+H_2O$	1.00E+13	0	1000
178	$N_2H_2+NO=N_2O+NH_2$	3.00E+12	0	0
179	$N_2H_2+NH=NNH+NH_2$	1.00E+13	0	1000
180	$N_2H_2+NH_2= NH_3+NNH$	1.00E+13	0	1000
181	$NH_2+NH_2=N_2H_2+H_2$	5.00E+11	0	0
182	$NO_2+O+M=NO3+M$	1.00E+28	-4.1	2470
	Enhanced third body efficiencies: N_2=O_2=1.5, $H_2$0=18.6, CO=2, CO_2=3			
183	$NO_2+NO_2=NO3+NO$	9.60E+09	0.7	20900
184	$NO_3+H=NO_2+OH$	6.00E+13	0	0
185	$NO_3+O=NO_2+O_2$	1.00E+13	0	0
186	$NO_3+OH=NO_2+HO_2$	1.40E+13	0	0
187	$NO_3+HO_2=NO_2+O_2+OH$	1.50E+12	0	0
188	$NO_3+NO_2=NO+NO_2+O_2$	5.00E+10	0	2940
189	$Na+N_2O$ = $NaO+N_2$	1.69E+14	0	3159
190	$NaO+H_2O$ = NaOH+OH	1.32E+13	0	0
191	$NaO+O$ = $Na+O_2$	2.23E+14	0	0
192	NaO+OH = NaOH+O	2.00E+13	0	0
193	$NaO+HO_2$ = $NaOH+O_2$	5.00E+13	0	0

194	$NaO+NO = Na+NO_2$	9.04E+13	0	0
195	$NaO+H_2 = NaOH+H$	1.25E+13	0	0
196	$NaO+H_2 = Na+H_2O$	3.13E+12	0	0
197	$NaO+CO = Na+CO_2$	1.00E+14	0	0
198	$Na+O_2+M = NaO_2+M$	1.74E+21	-1.3	0
	Enhanced third-body efficiencies:			
	H_2O=5, CO_2=3, CO=H_2=2			
199.	$NaOH+H = Na+H_2O$	5.00E+13	0	0
200.	$H+NaO_2 = HO_2+Na$	2.00E+14	0	0
201.	$NaO+H = Na+OH$	2.00E+14	0	0
202.	$NaO+OH = Na+HO_2$	3.00E+14	0	0
203.	$Na+HO_2 = NaOH+O$	1.00E+14	0	0
204.	$NaO_2+H = NaO+OH$	5.00E+13	0	0
205.	$NaO_2+OH = NaOH+O_2$	2.00E+13	0	0
206.	$NaO+HO_2 = NaO_2+OH$	5.00E+13	0	0
207.	$NaO_2+H = NaOH+O$	1.00E+14	0	0
208.	$NaO_2+CO = NaO+CO_2$	1.00E+14	0	0
209.	$NaO_2+O = NaO+O$	1.00E+14	0	0

Note: E: A units mole-cm- "sec-K, E units cal/mole"